77-1242 (R)

FILE CO
DO NOT REM

E-(49-1)-3800-7
Distribution Category UC-90g

DEVELOPMENT, TESTING AND EVALUATION OF MHD-MATERIALS

RECEIVED
DATE 7/21/77
OTP

Quarterly Report

for the period January - March 1977

H. P. R. Frederikse, T. Negas and S. J. Schneider

Inorganic Materials Division
Institute for Materials Research
National Bureau of Standards
Washington, D. C. 20234

Date Published: March 31, 1977

PREPARED FOR THE UNITED STATES
ENERGY RESEARCH AND DEVELOPMENT ADMINISTRATION
Under Contract No. E(49-1)-3800

"This report was prepared as an account of work sponsored by the United States Government. Neither the United States nor the United States ERDA, nor any of their employees, nor any of their contractors, subcontractors, or their employees, make any warranty, express or implied, or assumes any legal liability or responsibility for the accuracy, completeness, or usefulness of any information, apparatus, product or process disclosed, or represents that its use would not infringe private owned rights."

Table of Contents

Abstract

Efforts during this reporting period were directed primarily toward the design, fabrication, testing and pre- and post-test evaluation of real MHD electrode materials. Close collaboration was maintained with a number of MHD contractors and subcontractors with respect to procurement of specialized materials and their design. Additionally, NBS is involved with a number of MHD tests including the accelerated program of electrode testing in the MIT rig, the U-02 experiments, the AVCO tests utilizing slag and the UTSI/USSR tests. The evaluation/characterization of electrodes/insulators from five tests were completed and final reports were submitted. Several preheater refractories were also analyzed for Fluidyne Engineering Corp.

Progress in other areas included:

1. Viscosities of synthetic slags based on analyses of USSR coal ("Krushnitz") and "average" Montana Rosebud and Illinois #6 were measured.

2. The electrical conductivity of several oxide spinels was measured.

3. New measurements involving K-pressure over K_2O-SiO_2 solutions and a crystalline potassium zirconate were completed.

4. Chemical reactions in the K_2O-Al_2O_3-SiO_2-FeO_x system were investigated.

5. Mg-Al-Fe-oxide spinels were evaluated in terms of bonding to a metal substrate. Important chemical aspects of these oxides are discussed.

6. Evaluation of alloys for downstream components continued.

Objectives and Scope of Work

The overall objectives of this program are to obtain chemical and physical definition of high temperature materials which have shown promise for use in coal-fired open-cycle MHD power systems. Major problem areas in which investigations will be concentrated are:

1. Characterization of coal slag and its effects on system components and performance at prototype temperatures.

2. Development of electrode materials which provide adequate performance over extended periods of time.

3. Insulating materials which limit thermal losses and are resistant to prolonged thermal and erosion effects.

4. Preheater materials which can withstand the operating modes of separately and directly fired operation.

5. Seed recovery methods from slag which are technically and economically feasible.

6. Phase equilibria and diffusion rates of seed in slag and the corrosive action of combination on system components and materials.

7. Durability of prototype MHD sub-systems.

The program is designed to contribute to the solution of these problems by providing much needed data on candidate materials and by evaluating test samples and structures that have been subjected to real or simulated MHD conditions. The activities are grouped under six tasks:

G. Program Management Coordination (Assisting ERDA in coordination, planning and review of the various MHD-Materials Development Programs).

H. U-02 Materials Testing and Characterization (Coordination of U-02 Test Activities, Phase I). (Terminated June 30, 1976).

I. Operational Design Properties (viscosity, electrical conductivity, vaporization).

J. Corrosion by Seed and Slag (phase equilibria, diffusion).

K. Materials Testing and Characterization (test coordination, pre- and post-test analysis).

L. Assessment of Steam Plant Components (corrosion resistance of metals and alloys).

Summary of Achievements-Jan.-March 1977
(Completed Milestones - See Work Statement)

Progress of research and development in terms of the projected milestones of the NBS-ERDA contract are listed below. New priorities, particularly involving MHD materials testing and characterization, have resulted in the shifting of manpower as well as the modification of certain previous objectives. Many of the milestones also are continual in scope.

1a,b. Conducted negotiations with USSR concerning,
- a. Phase II, U-02 test
- b. A Phase III, U-02 test (Oct.-Nov. 1977)
- c. Materials Test, U-25 high B field
- d. USSR testing in US MHD facilities
- e. Fourth version of US/USSR MHD Status Report (Materials Division)

2. Participated in ERDA-MHD reviews, planning sessions, etc.

4. Measure viscosity of real slags. A USSR plus two US slags (synthetic, based on ash analyses) were measured.

5. Effect of oxide additions on viscosity. a) Effect of K_2O completed.

6. Effect of dissolved H_2O on viscosity. A high temperature-pressure viscometer has been constructed.

10a. Determined first version of the phase diagram for the "quaternary" system K_2O-Al_2O_3-SiO_2-FeO_x (seed-slag).

11a. Concluded measurements to determine the K-pressure over K_2O-SiO_2-Al_2O_3 solutions.

19. Measured the electrical conductivity of several spinels containing iron oxide and of arc plasma sprayed $LaCrO_3$ (MgO).

23. Measured seed vapor pressures for a portion of the K_2O-ZrO_2 system.

39a, 40a. Coordinated testing and/or conducted pre- and post-test analysis of electrode/insulator assemblies tested in various MHD facilities (ANL/Reynolds, AVCO, MIT, UTSI/USSR).

41,42. Assembled, updated and assessed data pertinent to corrosion of alloys in a downstream MHD environment.

Talks and Papers

F. A. Mauer, T. Negas, A. Perloff, E.N. Farabaugh, C. R. Robbins, "Analysis of MHD Electrodes and Coal Gasification Reactor Liners by Diffraction Methods", Session on Application of Diffraction to Fossil Fuel Energy-Related Materials, American Crystallographic Association, Feb. 23, Asilomar, Calif., Invited Talk.

T. Negas, "Chemistry of Ceramic Oxide MHD Electrodes", American Chemical Society Symp., Materials From a Chemical Viewpoint, New Orleans, March 22, Invited Talk.

H.P.R. Frederikse, "Electrical Conductivity of Mixed Spinels", American Physical Society Mtg., San Diego, Calif., March 1977.

Task G. PROGRAM MANAGEMENT AND COORDINATION (S.J. Schneider)

Program Review and Consultation Activities

S.J. Schneider participated in the regular ERDA-MHD staff meetings and in assorted program review/coordination meetings and briefings. The conclusions and recommendations resulting from these meetings are reflected in reports to ERDA or through direct consultation with ERDA staff.

NBS receives on a regular basis, MHD technical reports and proposals for review. During this period NBS provided 8 such evaluations.

Part of the NBS experimental program involves characterization of materials/component elements tested in various MHD test rigs and facilities throughout the United States (and USSR). In order to expedite the dessemination of this information, NBS has instituted a separate reporting system in addition to the regular Quarterly submissions. The system consists of the following elements: 1. Telephone report to submittor after initial examination, 2. Follow-up letter report, and 3. Detailed report (if warranted) to submittor and ERDA. The detailed report will be distributed to general contractors on an as needed basis as determined by ERDA; however highlights of the detailed report will be abstracted and published in the NBS Quarterly reports. In addition, general overall summary reports will be compiled from time to time and published in appropriate journals and special editions.

Inquiries regarding the status of any particular characterization or requests for additional assistance should be directed to:

A. Perloff 301-921-2900

(alternates)
T. Negas 301-921-2843
W. Hosler 301-921-2940

US-USSR Cooperative Program

1. U-25 Electrode Program

The major bulk of this activity has been completed by the participating contractors. Henceforth, certain aspects of the program will be continued although at a somewhat less accelerated pace. NBS responsibilities and accomplishments are reported elsewhere in this report.

2. US-USSR Materials Program Activities

During this reporting period, the US-USSR Ad Hoc Materials Working Group held its first 1977 meeting in Washington, D. C. Agenda items included: 1. Phase II U-02 materials test (final draft report now in preparation), 2. Phase III materials test on U-02 (agreement reached to conduct test in Oct.-Nov. 1977), 3. Materials test on U-25 high B field facility (preliminary discussion only with no firm commitments made), 4. USSR materials in US MHD facilities (Phases I and II at UTSI completed; tentative plans laid for similar testing at Westinghouse in the latter part of 1977), and 5. Joint US-USSR chapter on materials (Status Report) (fourth revision agreed to by US-USSR authors).

Task I. OPERATIONAL DESIGN PROPERTIES

a. Viscosity of Coal Slags (W. Capps and D. A. Kauffman)

Introduction

Part of the program of characterizing MHD materials is the preparation of synthetic slags and the determination of viscosity of these and any real slags furnished to NBS by other contractors.

In the past, six real combustor slags and one MHD channel slag have been measured and seven artificial slags based on real ash analyses have been made and measured. This service to the MHD community will be continued.

Slag Preparation and Viscosity Measurements

1. A synthetic slag based on a chemical analysis of a "standard" USSR coal slag (called Krushnitz) was prepared. It is relatively high in SiO_2 and Al_2O_3 and low in Fe_2O_3 and CaO. Its viscosity is correspondingly high (K-864). The analysis was obtained from Dr. Crawford of UTSI. The viscosity and analysis are shown in Fig. 1.

2. A list of approximately 160 analyses of Montana Rosebud coal together with an average analysis for the whole lot was obtained from Dr. Postelthwaite of ERDA-Fossil Energy. The analyses were made on core samples from a large area of the mine in Colstrip, Montana. An "average" Montana Rosebud slag was made and measured (K-875). This made a very stable melt which did not crystallize at temperatures as low as 1142 °C. See Fig. 1.

3. A series of analyses of ashes from Illinois #6 coal was also "averaged". These were obtained by ERDA from PERC. Melt number K-879 simulates this average Illinois #6 slag. See Fig. 1.

4. The above mentioned average Rosebud and Illinois #6 analyses are quite similar except with regard to CaO and Fe_2O_3 concentrations. For systematic laboratory investigations, it is desirable to minimize the number of melts while realizing a maximum amount of data. Therefore with increased emphasis on working with "standard" slags a new standard or "base" composition was devised which is intermediate between the Rosebud and the Illinois #6. This base is identified as K-884 in Fig. 2. Systematic variations will be made by increasing or decreasing each constituent oxide in turn in discrete increments.

The data will be very useful in developing a nomogram type of calculation method for predicting viscosity using temperatures and composition as independent variables. Increments of SiO_2 of 5, 10 and -5% have already been made. See Fig. 2. These are K-887, K-901 and K-913, respectively. Future melts will be made varying Al_2O_3, Fe_3O_4, CaO and MgO.

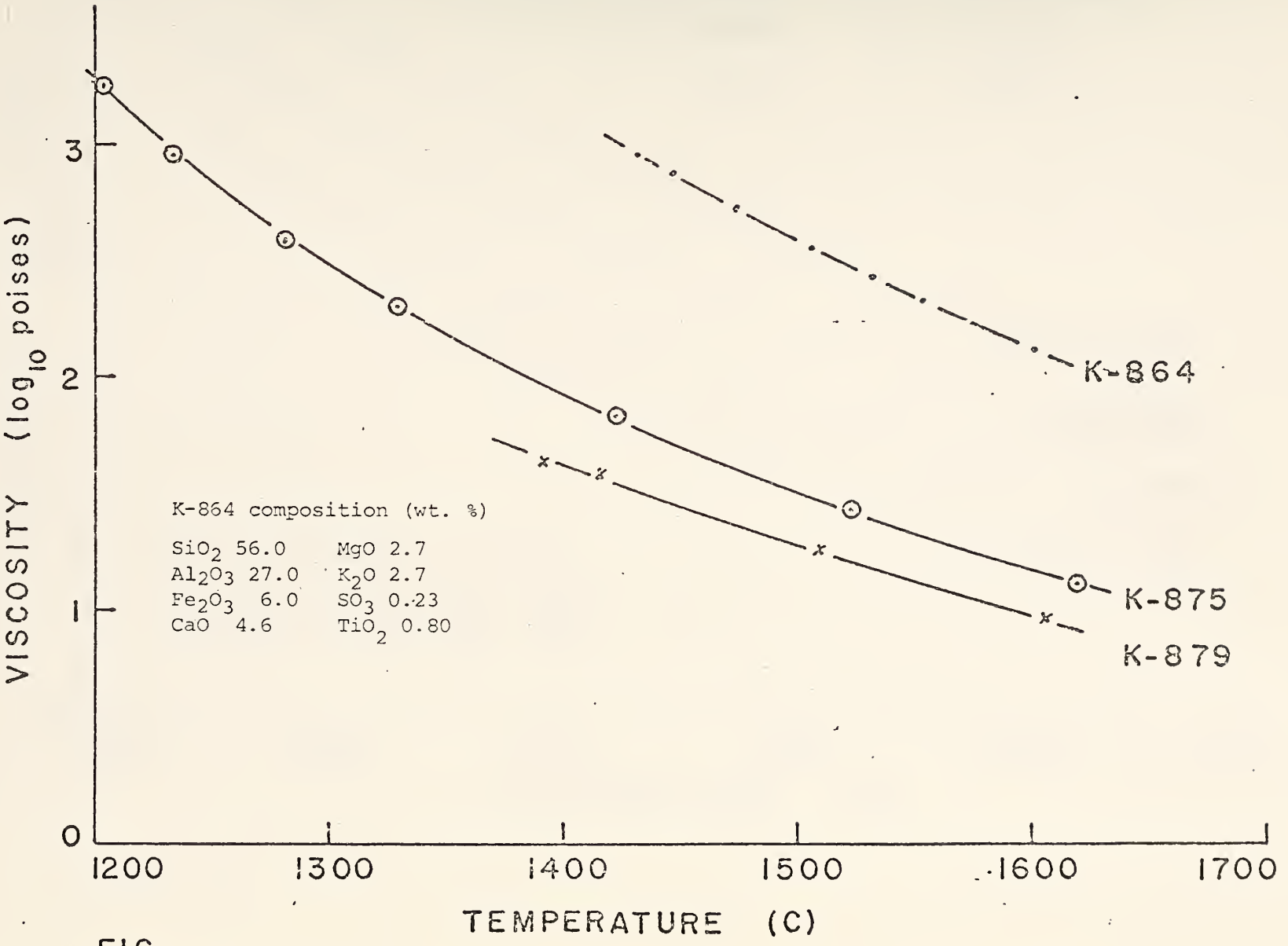
VISCOSITY (log10 poises)
3
2
1
0
1200
1300
1400
1500
1600
1700
TEMPERATURE (C)
K-864
K-875
K-879
K-864 composition (wt. %)
SiO2 56.0
Al2O3 27.0
Fe2O3 6.0
CaO 4.6
MgO 2.7
K2O 2.7
SO3 0.23
TiO2 0.80

FIG. 1.

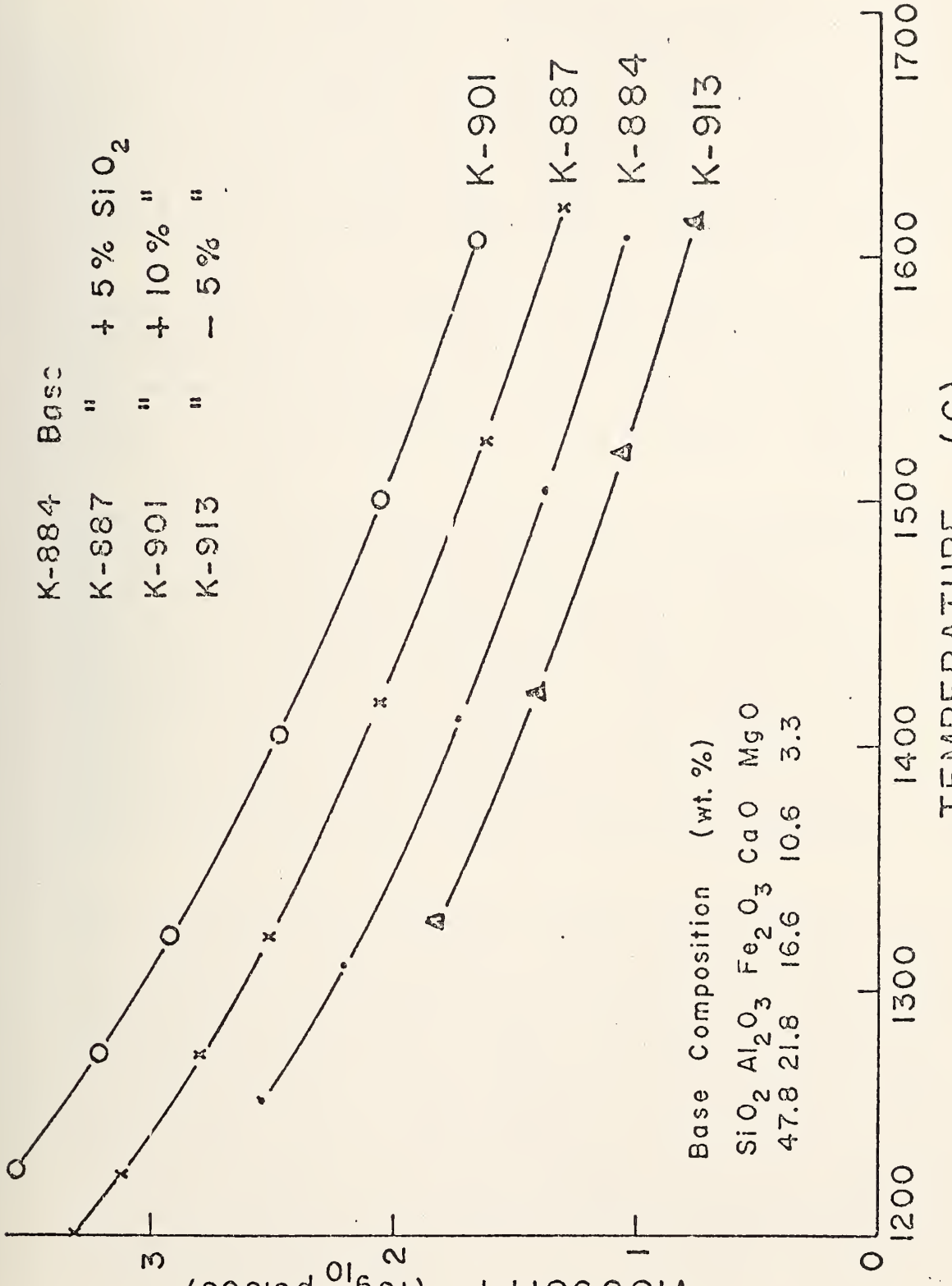
K-884 Base
K-887 " + 5% SiO2
K-901 " + 10% "
K-913 " - 5% "
K-901
K-887
K-884
K-913
Base Composition (wt. %)
SiO2 Al2O3 Fe2O3 CaO MgO
47.8 21.8 16.6 10.6 3.3
VISCOSITY (log10 poises)
TEMPERATURE (C)
0
1
2
3
1200
1300
1400
1500
1600
1700

FIG. 2.

b. Electrical Conductivity (W. R. Hosler and A. J. Armstrong)

We have measured the electrical properties of nickel aluminate ferrous ferrite. These particular samples were composed of $17NiAl_2O_4$-$3Fe_3O_4$ and are designated at NAFF 173. The original billet was pressed and sintered at 1548 °C for 7 hours at which time it was cooled slowly in N_2. The sample taken from this billet is designated 7756. The electrical conductivity shown in Fig. 3 is low and oxygen pressure dependent. Apparently, oxidation of the iron at the lower temperatures and higher O_2 pressures causes the considerable decrease in conductivity. This sample was 74.5% of theoretical density and displayed many cracks after the completion of the measurement. These cracks were probably caused by the iron oxidation toward an Fe_2O_3 phase.

A second billet was pressed and fired at 1560 °C for 6 hours and cooled in N_2. This billet had a density of 86.6% theoretical. Electrical data on a sample from this billet is shown in Fig. 3 also and designated as 7760. The electrical conductivity is higher than the less dense sample as expected and the oxygen pressure dependence is less. NAFF 173 or some other proportion of nickel aluminate and iron oxide might be a promising electrode material especially in a slagging environment where SiO_2 would be a problem with most materials.

Fig. 4 gives the electrical conductivity as a function of reciprocal temperature of magnesium aluminate ferrous ferrite ($MgAl_2O_4$-Fe_3O_4) called MAFF 11. The data for reducing conditions (10^{-6} O_2) was taken first. As can be seen from the data the conductivity is excellent and the slope is relatively flat. A room temperature value of conductivity after the run was 5×10^{-2} $(\text{ohm cm})^{-1}$. No oxidation occurred at the lower temperatures. However, at 10^{-3} O_2 partial pressure rapid oxidation occurs even at 1100 °C and in air the oxidation starts as high as 1400 °C. Indications are from this data that the material would not be suitable for an MHD electrode except as a graded component at very low temperatures, i.e., less than 500 °C. Even in this case the conductivity at room temperature of 5×10^{-2} $(\text{ohm cm})^{-1}$ is not considered excellent for a joule heating face MHD electrode. This sample was 74.4% theoretical density. Further sintering and densification would probably increase the conductivity of this material and its resistance to oxidation.

Preliminary measurements have been made on arc plasma sprayed $LaCrO_3$-.05Mg. While the conductivity is adequate for MHD power generation >1.0 $(\text{ohm cm})^{-1}$, it is considerably less than that of the sintered $LaCrO_3$-Mg samples measured and reported in the July-Sept. 1976 quarterly report. This particular sample was cut from a demonstration piece made to show the feasibility of arc plasma spraying $LaCrO_3$ and its $MgAl_2O_4$ insulator to a considerable thickness. The $MgAl_2O_4$ insulator side was sprayed to a depth of approximately 3 mm. The $LaCrO_3$ was attached (sprayed) directly to the insulator to a depth of another 7 or 8 mm and finally the last insulator side was sprayed to the $LaCrO_3$ to another 3 mm so that the total sandwich is 13 to 14 mm thick. The sample was cut from this sandwich and had the insulator side in tact during measurement. No density measurements have been made on this particular piece but some increase in conductivity as a function of time at high temperature was evident which probably indicates that sintering was occurring. Additional details will be given in the next report.

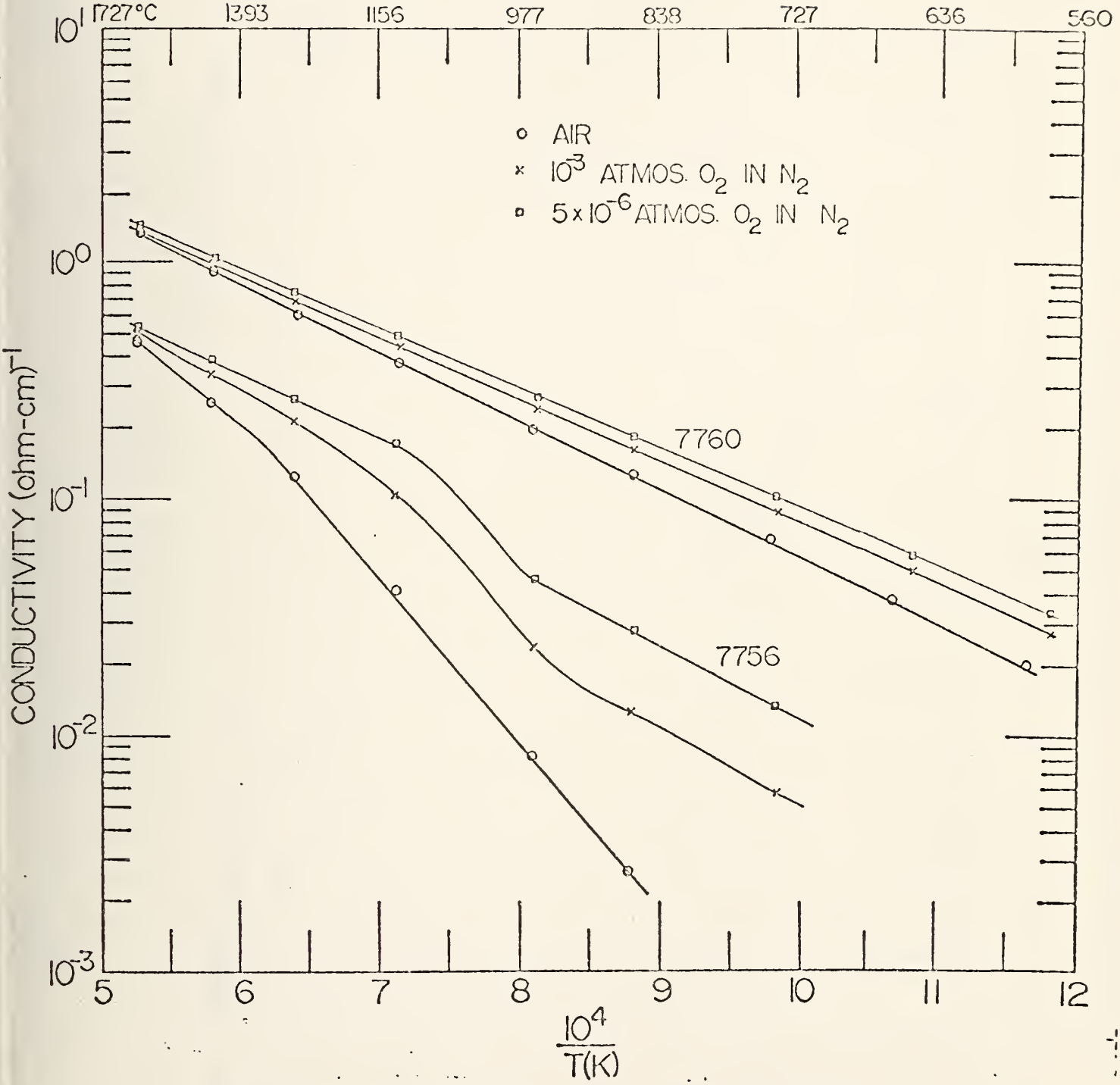

Fig. 3. Electrical conductivity vs. reciprocal temperature for $17NiAl_2O_4$-$3Fe_3O_4$ (NAFF 173) for several partial pressures of oxygen. 7756 is 74.5% dense - 7760 is 86.6% dense.

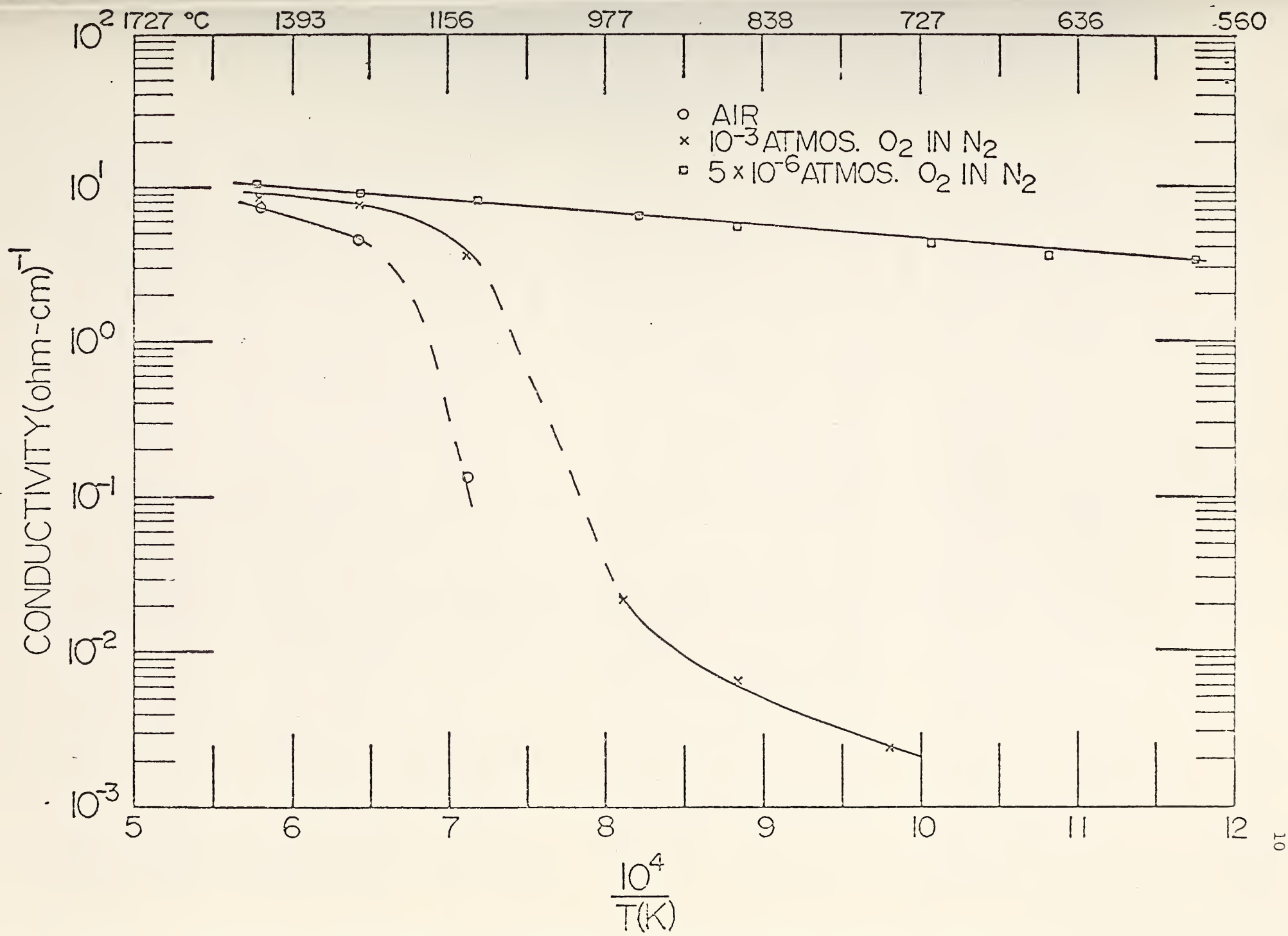

Fig. 4. Electrical conductivity vs. reciprocal temperature of $MgAl_2O_4$-Fe_3O_4 (MAFF 11) for several partial pressures of O_2

c. Vaporization Studies (E. R. Plante)

This section describes measurements of the potassium gas pressure over K_2O-containing compounds or phases. Such data is of critical importance in predicting the extent of interaction of the seeded MHD plasma with construction materials or coal ash. During this quarter measurements were completed on the vaporization of K_2O dissolved in silica, new vaporization data were obtained on $K_4Zr_5O_{12}$, and measurements on a glass composition which contains K_2O, SiO_2, and Al_2O_3 were begun. All data were obtained by mass spectrometry using the observed weight loss of K_2O for calibration purposes when possible.

K_2O-SiO_2 Measurements

In the last quarterly report (1) vapor pressure data for K were reported over the composition range 43.9 to 11.9 wt% K_2O in SiO_2 solutions. During this reporting period these measurements were concluded. Vaporization measurements were terminated at a calculated composition of about 6.8% K_2O when non-saturation effects became apparent. During the final period of the experiments stress relief in the furnace caused buckling to occur which resulted in local hot spots in the Knudsen cell. As a result, some platinum was vaporized from the cell and a valid calibration constant for these measurements could not be determined. However, calibration constants previously determined in this work were sufficiently reproducible that an average value based on the previous calibrations is probably correct to within 10-20% so an average value was used. The data for this composition range (11.9 - 6.8 wt% K_2O) was fit by least squares to give the equation,

$$\log P_K(\text{atm}) = (3.841 \pm .076) - (14654 \pm 116)/T + (52.76 \pm 4.26)N^2$$

where N is the mole fraction of K_2O in the solution. The coefficients in this equation differ somewhat from the data obtained previously in this series especially with respect to the coefficients for the 1/T and N^2 terms. It has not yet been determined how well this data fits the equation covering the composition range from 43.9 to 11.9 wt% K_2O. As noted in the last quarterly report these measurements do not pertain to equilibrium as represented on an equilibrium phase diagram. In addition, it must be noted that the treatment of the data assumes a homogeneous glass or melt is present in the effusion cell for the determination of the mole fraction of K_2O in the solution. These points require further investigation. However, it should be noted that the amount of seed capture possible at these low concentrations is far less important to MHD than the higher concentration ranges.

Comparison of the current data with previous mass spectrometric data obtained using the TOF mass spectrometer shows excellent agreement at 20 wt% K_2O with poorer agreement at higher K_2O content. The ratio of the potassium pressure observed using the TOF spectrometer to that observed using the quadrupole mass spectrometer is 1.10, 1.25, 1.5, 1.8, 2.3 and 3.2 at 1725K and 20, 25, 30, 35, 40 and 45 wt% K_2O respectively. The cause of the difference between the TOF data and quadrupole data at

45 wt% K_2O is surprisingly large and is not understood. It is believed to result, however, from unknown differences in the samples or temperature measurement rather than differences in the mass spectrometers used.

"$K_4Zr_5O_{12}$" Measurements

Because of the importance of zirconia as an MHD construction material, measurements were carried out of the potassium pressure produced by the reaction:

$$1/2K_4Zr_5O_{12}(c) = 2K(g) + 1/2O_2(g) + ZrO_2(c).$$

These measurements help to define the temperature and overpressures of K and O_2 which can be tolerated by zirconia without compound formation. The compound $K_4Zr_5O_{12}$ (composition nominal until proven by a structure analysis) is the most stable, easiest to prepare phase in the K_2O-ZrO_2 system.

Pressures were measured using the quadrapole mass spectrometer and Pt effusion cells with the temperature monitored by a Pt-Pt (10% Rh) thermocouple. Several sets of data were obtained but the results are not entirely unambiguous because of possible interference from residual K_2CO_3 at the beginning of the experiments and the possibility that the reaction is slow because of complicated crystal chemistry. Data were obtained with crucibles having orifice diameters of .020" and .0135". If the mass spectrometer constant did not change appreciably the product kac, where k is the observed mass spectrometer constant, a is the orifice area, and c is the Clausing factor for the orifice, would be constant. Failure to obtain this consistency makes it appear likely that leakage of vapor from around the cell lid took place during the measurements made with the smaller orifice diameter. The potassium pressure based on what appears to be the most realiable set of data is:

$$\log P_K(\text{atm}) = -14133 \pm 106/T + 6.248 \pm .106$$

Further analysis and the implications of these results with respect to compound formation because of seed interaction with zirconia will be differred to a future report.

K_2O - SiO_2 - Al_2O_3 Measurements

Measurements of the K pressure over the three component system are in progress. Preliminary data have been obtained on a sample designated K210 which was obtained from the Geophysical Laboratories, Washington, D. C. and is among the well characterized K_2O-SiO_2-Al_2O_3 glasses used by Schairer and Bowen (2). Previous attempts to measure the K pressure over several of these glasses at NBS were made using a microbalance system but without success.

The starting composition of K210 was 39.6% wt% K_2O, 10.0% Al_2O_3 and 50.4% SiO_2. Thus far a number of vaporization experiments have been run using a Pt effusion cell with a 1/2 mm diameter effusion hole. A number of preliminary results can be briefly stated. The initial K pressures observed at about 39% K_2O content are 3 to 4 times higher than the pressures of K currently accepted as "best" for K_2O-SiO_2 solutions at 40 wt% K_2O, i.e., the results using the quadrapole spectrometer reported in the last quarterly report (1). The slopes of $\log P_K$ versus 1/T are less steep for the alumina containing solutions than for the K_2O-SiO_2 solutions and appear to become less steep as the K_2O evaporation proceeds. The potassium pressure decreases faster with decreasing mole fraction of K_2O than for the solutions containing only K_2O and

SiO_2. An equation of the type $\log P_K = B0 + B1/T + B2 \cdot N^2$ with N the mole fraction of K_2O in the melt, which fit the K_2O-SiO_2 solution data over the range from 44 wt% to 11.9 wt% K_2O very well, gives a poor fit to the present data over the range from 39% K_2O to 28% K_2O.

Future Work:

During the next quarter, measurements on the K pressure over K_2O-SiO_2-Al_2O_3 solutions will be continued. The amount and reliability of the data for the K_2O-SiO_2 solution case is sufficiently good so that the implications of this data to seed capture for a pure solica-K_2O "slag" will be examined and reported.

References

1. NBS Quarterly Report, December 1976.

2. J. F. Schairer and N. L. Bowen, Am. J. Sci. 253, 681 (1955).

Task J. Corrosion and Diffusion

A. Seed-Slag Interactions

a. The System K_2O-Al_2O_3-SiO_2 (L. P. Cook, J. L. Waring, R. S. Roth and C. A. Harding)

During the past quarter a graphite furnace has been installed and tested which will allow experiments to be conducted at temperatures up to 2700 °C in an inert atmosphere. $Pt_{60}Rh_{40}$ tubing has been found to be useable up to ~1920 °C if care is used in annealing prior to welding.

Further experimentation has been conducted to determine the melting point of $KAlO_2$. The melting point appears, on the basis of experiments in an inductively heated iridium crucible, to be considerably higher than previously estimated (Ref. 1). A series of experiments at 1750 °C showed no melting for compositions richer in $KAlO_2$ than $58KAlO_2$:42 SiO_2 in agreement with our preliminar experiments, as given in a previous quarterly report (Ref. 2).

Molybdenum and tantalum tubing have been ordered and received. These materials will be tested for use in sealed quench experiments above 2000 °C. A controlled atmosphere facility for loading and welding experiments is being assembled.

b. The Slag System CaO-K_2O-MgO-Al_2O_3-SiO_2-"FeO" (L. P. Cook, C. L. McDaniel and T. Negas)

The six component system described above provides a working model for "real" MHD slag (Ref. 3). The experimental approach to be used has been outlined in a previous quarterly report (Ref. 4).

A controlled atmosphere facility with analytical balance has been installed and placed in operation. Using this facility, starting materials are being prepared as shown in Fig. 1. During the next quarter experiments will be begun to determine liquidus temperatures in the indicated binary systems. Analytical expressions relating composition to liquidus temperature will be derived from these data. These expressions will be used to guide experimentation in more complex, multicomponent systems.

References

1. F. E. Spencer, J. C. Hendrie, Jr. and D. Bienstock, Sixth Intl. Conf. on MHD Electrical Power Generation, Vol. II, Washington, D. C. 1975, p. 202.

2. H. P. R. Frederikse, T. Negas and S. J. Schneider, NBS Quarterly Report, October - December 1976, p. 21.

3. H. P. R. Frederikse, T. Negas and S. J. Schneider, NBS Quarterly Report, April - June 1976, p. 30.

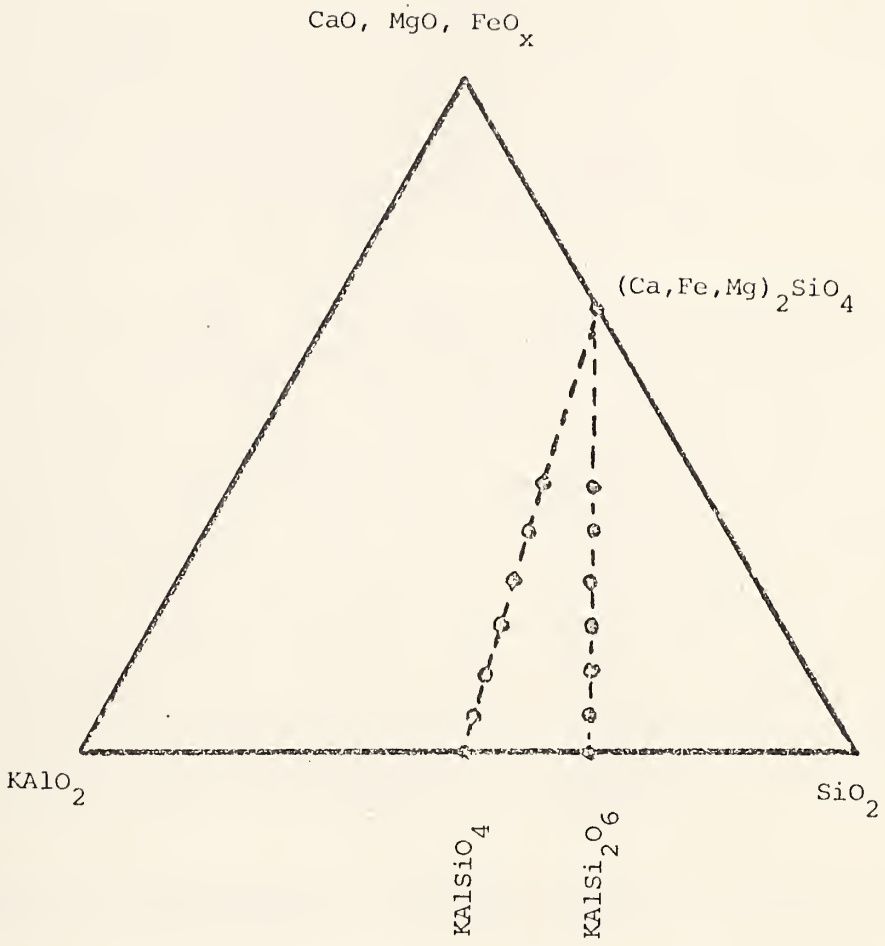

Fig. 1. Synthetic Slag Compositions for Experimental Investigation

c. The System $KAlO_2$-$KAlSiO_4$-"FeO_x" (Han Ill Yoo, guest worker from the Korean Standards Research Institute, R. S. Roth and T. Negas)

As part of our program to elucidate chemical processes involving slag components the "quaternary", K_2O-Al_2O_3-"FeO_x"-SiO_2, is now under investigation. Ten specimens were prepared as indicated in Fig. 2. These were equilibrated in sealed Pt-tubes, quenched, and examined by X-ray diffraction. It was determined that the subsystem $KAlSiO_4$-"FeO_x" is "binary" as indicated by Fig. 3. However, the $KAlO_2$-"FeO_x" tie-line is not "binary". The $KAlO_2$-$KAlSiO_4$-"FeO_x" compositional triangle, therefore, is not ternary. Specimens react to form a $KAl_{1-x}Fe_xO_2$-type solid solution plus a β-alumina type compound containing a high percentage of iron oxide.

These preliminary data demonstrate several types of reactions to be expected among, for example, Fe/Al-oxide construction materials and slag components plus seed. Simultaneously the chemical behavior of slag plus seed combinations can be elucidated. For example, consider the $KAlSiO_4$-"FeO_x" system in Fig. 3. Starting Fe/Al ratios and K/Si-oxide contents are varied by the two components $KAlSiO_4$ (a common crystalline phase in MHD slags) and FeO_x. Noteworthy are the subsolidus equilibrium assemblages $KAlSiO_4$ + Fe_2O_3 (hematite) and $KAlSiO_4$ plus Fe_3O_4 (magnetite). The latter exists only above ∿1425 °C under oxidizing conditions. This temperature ($Fe_2O_3 \leftrightarrow Fe_3O_4$ equilibrium) will be displaced toward lower temperature with decreasing P_{O_2}. The presence of Fe_3O_4 (which is a highly conductive spinel) as an equilibrium product in slag may contribute to axial leakage in a slagging MHD generator. The more extensive (compositionally) system $KAlSiO_4$-$KAlO_2$-"FeO_x" suggests that K-β-alumina phases (containing iron oxide as well as Al_2O_3) are expected corrosion products of Fe/Al-oxide construction materials. These β-alumina phases probably are mixed ionic/electronic conductors and are under investigation as part of a project independent of this MHD program.

B. Diffusion in Slag-Insulator and Insulator-Electrode Couples (A. J. Armstrong, E. N. Farabaugh and J. R. Manning

Because of the continuing interest in spinel materials for MHD insulator and electrode applications, research has been planned which will lead to the determination of diffusion profiles resulting from slag-insulator and insulator-electrode reactions at various temperatures and times. Changes in composition resulting from diffision may strongly affect the electrical, insulating and conducting properties of spinel materials.

We have chosen Illinois #6 as the slag to be used in this work, since Illinois #6 has been selected as the representative eastern coal. A specimen of the slag has been cut, polished and examined by SEM and EDX techniques to document the elemental constitution and microstructure of an untested slag sample. The slag was found to be composed of Mg, Al, Si, K, Ca, Ti and Fe as is shown in Fig. 4, an EDX spectrum taken from the slag. This elemental analysis is identical with that found for larger specimens of slag, thus indicating a reasonably homogeneous slag material. We have characterized the slag this reporting period and will fabricate slag-insulator couples and study them next reporting period.

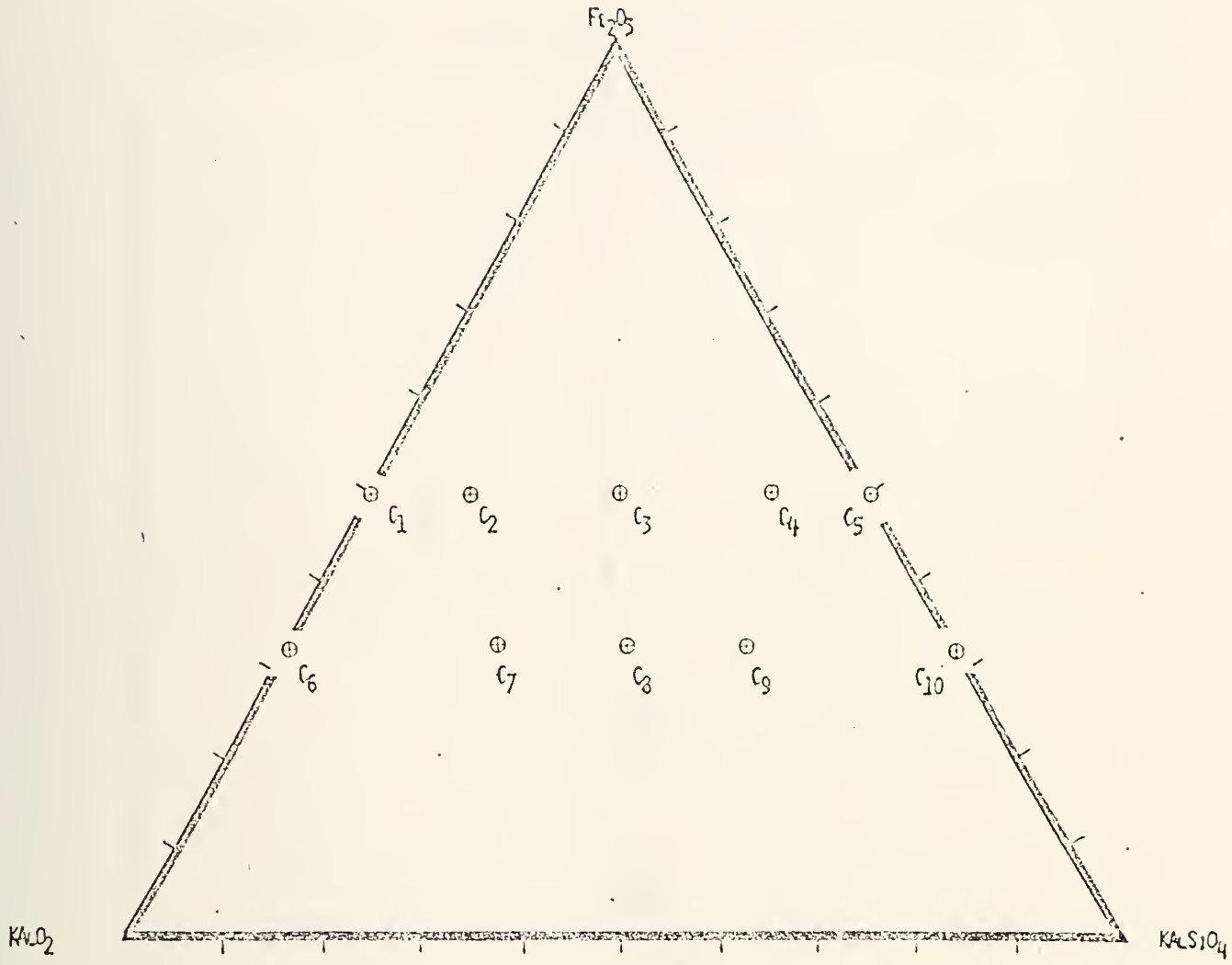

Fig. 2. Specimens Investigated in the $KAlO_2$-$KAlSiO_4$-FeO_x (plotted as Fe_2O_3) compositional triangle.

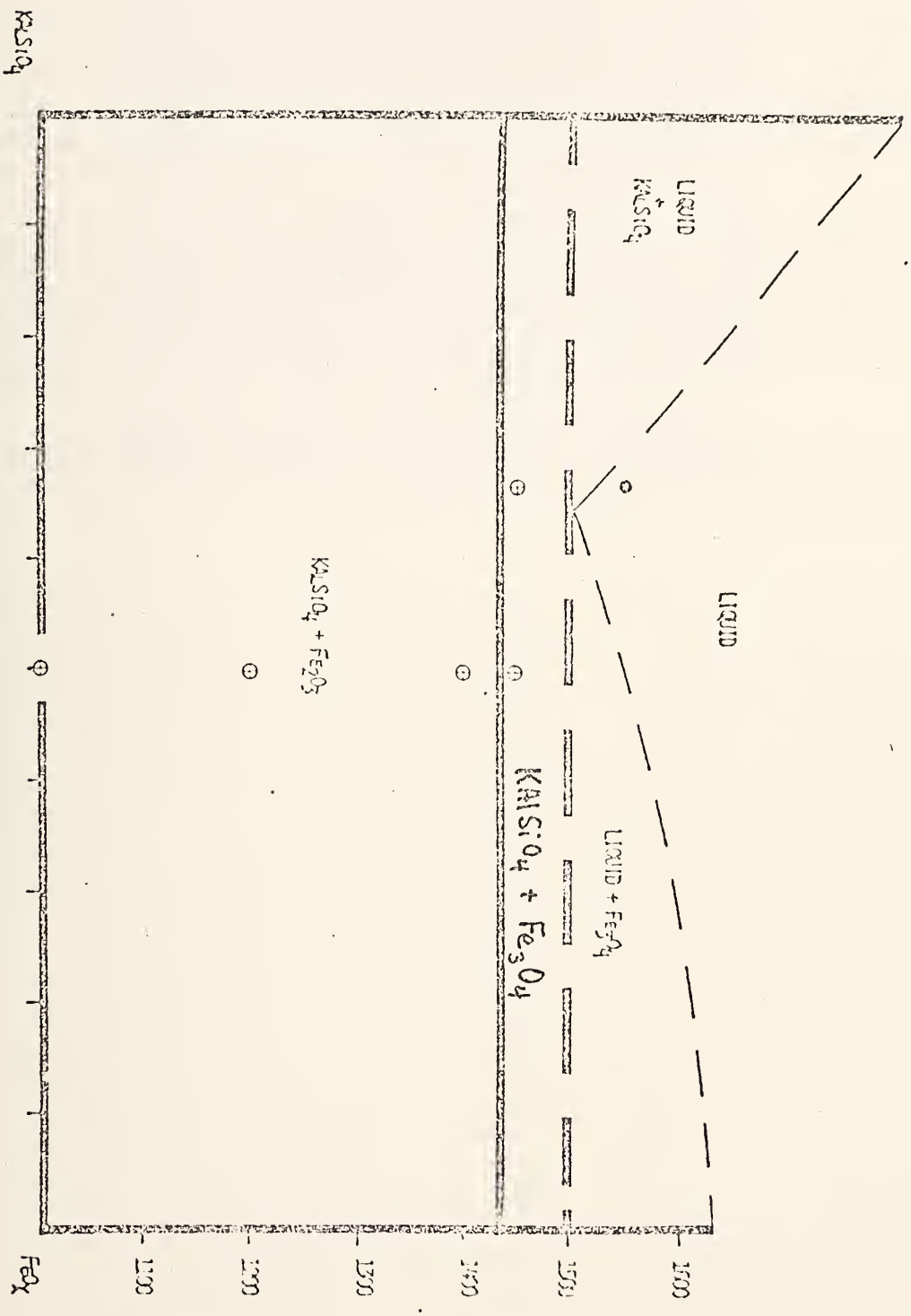

Fig. 3. Preliminary phase diagram for the $KAlSiO_4$-FeO_x system, in air.

Various insulator materials, $MgAl_2O_4$, MgO and Al_2O_3 have been used in the formation of insulator-electrode couples. The electrode material used was MAFF-31 ($3MgAl_2O_4 + Fe_3O_4$). These couples were assembled by first wrapping the insulator specimen with 0.001" platinum wire, pressing the insulator between two larger pieces of material (either slag or electrode samples) and clamping the diffusion couple between two Al_2O_3 plates. The Al_2O_3 plates are held together with thick platinum wire and sufficient tension is induced to provide some compression of the diffusion couple. The thin platinum wire, which is wrapped around each insulator specimen, provides a boundary marker for the insulator edge. This construction is shown in Fig. 5.

In the next reporting period, it is planned to heat these insulator-electrode couples at 1600 °C for 1, 10 and 100 hrs. With the use of diffusion boundary markers, it is anticipated that the problem of determining the position of the insulator-electrode interface, described in an earlier report, will be eliminated, thus allowing good Fe diffusion profiles in the insulator to be determined.

Slag-insulator couples will be made and treated at 1300 ° - 800 °C for 1, 10 and 100 hrs. during the next period. Penetration of different slag constituents into the three insulator materials will be investigated.

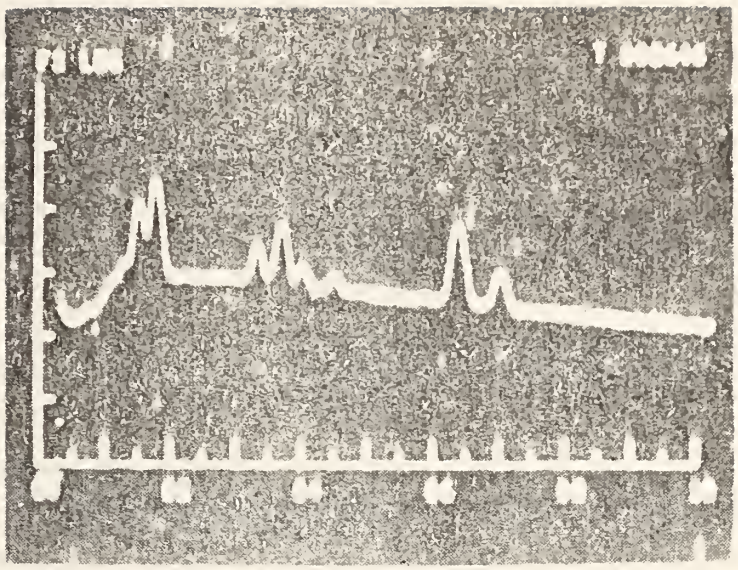

Fig. 4. EDX from Illinois #6 slag.

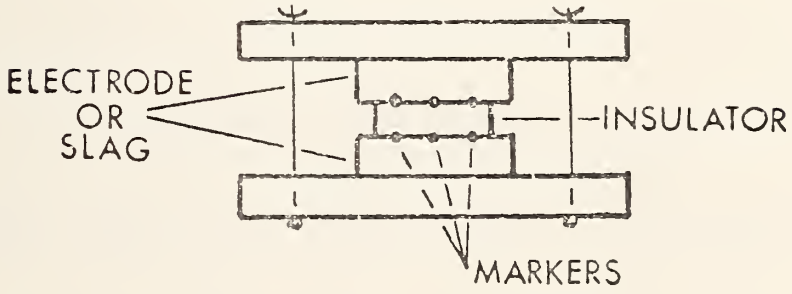

Fig. 5. Typical Diffusion Couple Experiment Rig.

Task K. Materials Testing and Characterization

A. U-02, ANL, MIT and AVCO Programs

1. U-02, Phase II (T. Negas)

As indicated in the previous Quarterly Report, analyses of U-02, Phase II electrodes were completed and a final report was under preparation for Westinghouse Corp. This report is rather extensive and will not be reproduced here. However, the summary below illustrates the scope of the work.

Radiography, powder X-ray diffraction and high magnification SEM combined with EDX analysis served as the dominant analytical methods. The report is divided into the following sections,

I. Introduction
   A. Handling of the Module
   B. Scope of this work

II. General Features of the Module
   A. Environmental Contaminants
   B. Mobility of Iron and Chromium
   C. Metal Leadout Zones and MgO Insulators

III. Post-Test Chemistry of Materials
   A. Mg-Al-Fe Oxide Solid-Solution Spinels
   B. "Hercynite"-Based Spinel Electrodes
   C. $LaCrO_3$ (Mg) and Cerium Oxide-ZrO_2

IV. Conclusions

Eighty-seven figures are included. The following conclusions, not necessarily in order of importance, can be summarized based on our analyses.

1. Excessive but interrelated thermal-mechanical-electrical stresses were the most important factors influencing the performance of the module.

a. These combined to cause degradation of side insulators, leadout materials and leadout zones including underlying MgO blocks.

b. In turn, original thermal parameters deviated toward higher temperatures from original design. Overheating at leadout zones is apparent for many electrodes, heat being dissipitated probably via the MgO insulation.

c. The chemical integrity of materials, therefore, was compromised by excessive, localized heating.

d. Intrusion of seed enhanced further mechanical and chemical deterioration via reactions including solution and probable electrochemical action.

2. MgO insulation for electrodes containing high iron-oxide contents is not suitable for temperatures designed to exceed 1700 °C.

3. The iron oxide-containing materials should be limited to applications below ~1700 °C. The "hercynite"-based spinels should be utilized probably below 1600 °C.

a. The "hercynite"-based electrodes should remain in high density form to prevent,

1. exsolution reactions and reactions with seed.

b. The Mg-Al-Fe-oxide electrodes should have better conductivity at leadout temperatures wherein oxidation and exsolution to resistive phase can occur. (See extended discussion of the chemistry of MAFF-31 in this Quarterly Report.)

4. $LaCrO_3$-based electrodes are encouraging although evidence for vaporization of Cr-oxide(s) and solution by seed is abundant. $LaCrO_3$ or other related perovskites could be an effective leadout material.

5. Alternate methods of fabricating the Mg-Al-Fe-oxide spinel should be explored to prevent segregation of impurities at grain boundaries.

2. ANL/MIT Testing

a. NBS/Trans-Tech Tests (W. R. Hosler)

During this reporting period several tests were carried out in the MIT test rig. The first test was made on January 14, 1977 and the electrodes tested consisted primarily of magnesium aluminate ferrous ferrite (MAFF 31) fastened to a Hastelloy B base through a cermet grade. The MAFF 31 had a yttria stabilized zirconia cap. The Hastelloy B was brazed directly to the standard MIT test rig base.

The electrode was designed for a heat flux of 100 watts/cm^2 and with allowance for temperature excursions of 200 °C at the plasma electrode interface. The design temperatures were:

1830 °C surface
1300 °C $ZrO_2(Y_2O_3)$-MAFF 31 bond line
550 °C cermet bond line
50 °C copper-Hastelloy B bond line

Using the appropriate thermal conductivities of the materials involved, the thicknesses were:

$ZrO_2(Y_2O_3)$	0.70 mm
MAFF 31	2.04 mm
Hastelloy B	6.75 mm

The test lasted a total time of 1 hour, 47 minutes and was terminated because it became apparent that no more useful information could be obtained.

Almost immediately upon ignition, the magnesium aluminate plate insulators popped out into the plasma stream about 3 to 8 mm. From the start, the ZrO_2 caps began coming off in areas and were almost entirely gone at 15 minutes into the run. During the electrode set-up no particular precautions were taken to keep the ceramics dry. In addition, the test date was an extremely cold day in Boston and the gas stream scrubber on the roof froze. At start-up a malfunction occurred and water streamed down over the electrodes. While a heat gun was trained on the system for a short while before ignition, the

ceramics may have still contained some moisture. Even with the above difficulties, the electrode functioned well and application of current continued according to a pre-arranged plan. The electrodes were returned to NBS where they are being examined in detail. A more detailed report will be made later.

A second test was carried out on the MIT test rig on February 18. These electrodes were made of lanthanum chromite which was arc plasma sprayed on the standard MIT test rig base. A yttria stabilized ZrO_2 cap was sprayed on the $LaCrO_3$. A schematic design is shown in Fig. 1. Before ignition extreme care was taken to keep the electrodes dry. They were kept under an infrared heat lamp until the chamber was closed and cooling water was not run through the electrodes until 15 to 30 seconds before ignition of the pilot burner.

Ignition of the main burner was accomplished with a good cold start which minimized shock to the electrodes. The caps and electrode insulators which were magnesium aluminate sprayed directly on the electrode side functioned well. All caps remained in place except a small central portion of the lower cathode which oblated away during the run. The run lasted for 3 hours and 52 minutes with a total time under power of 2 hours, 41 minutes. No arcing was observed on any electrode at any time and the current voltage relationships indicated a soft electrode condition, i.e., voltages were not high to maintain the current densities of 1.5 a/cm^2. During the test we observed a loosening of the bond between the copper electrode base and the $LaCrO_3$ at the outer electrode edges. After the run the anode and cathode sections were clamped in their positions for transport to NBS for analysis. The loosening of the $LaCrO_3$-Cu bond appeared to be the most serious difficulty. It is impossible to determine how much loosening was done during the run and how much happened during and after cool down. Generally, the electrodes functioned well, and an electrode incorporating this design appears promising.

A detailed analysis is being carried out now and a report will be available.

b. SEM and EDX Examination of ANL"Dummy"Electrodes (E.N. Farabaugh)

Sections were cut from the dummy electrodes which revealed typical cross sections from relatively undamaged areas and from severely eroded areas of the electrode. A detailed report, summarized below, is available.

The electrodes consisted of a ZrO_2 cap on top of a Ni-Cr-Al alloy layer which, in turn, was on top of stainless steel. The stainless steel was joined to a copper cooling strip. It was noted that the copper cooling strip came free from the stainless steel in most cases. There was no evidence, however, of separation at either the ZrO_2 - alloy or alloy-stainless steel interfaces.

The electrode, #101, with the thickest ZrO_2 cap ($\sim$1 mm) withstood the testing better than those with thinner caps. There was some ZrO_2 left in the severely eroded areas of 101 while 102, 201 and 202 retained little or no ZrO_2 in the severely eroded areas. All the electrodes with ZrO_2 caps $<$1 mm thick suffered damage to a depth of .5 to .6 mm below the bottom of the ZrO_2 cap. New Fe-Si-K phases were formed in the damaged areas.

The Al in the alloy layer (the layer was $\sim$.1 mm thick) often appeared in the form of elongated islands in the Ni-Cr-Al phase. In some cases with thin ZrO_2 caps, the thickness of the alloy layer was reduced in the heavily eroded areas.

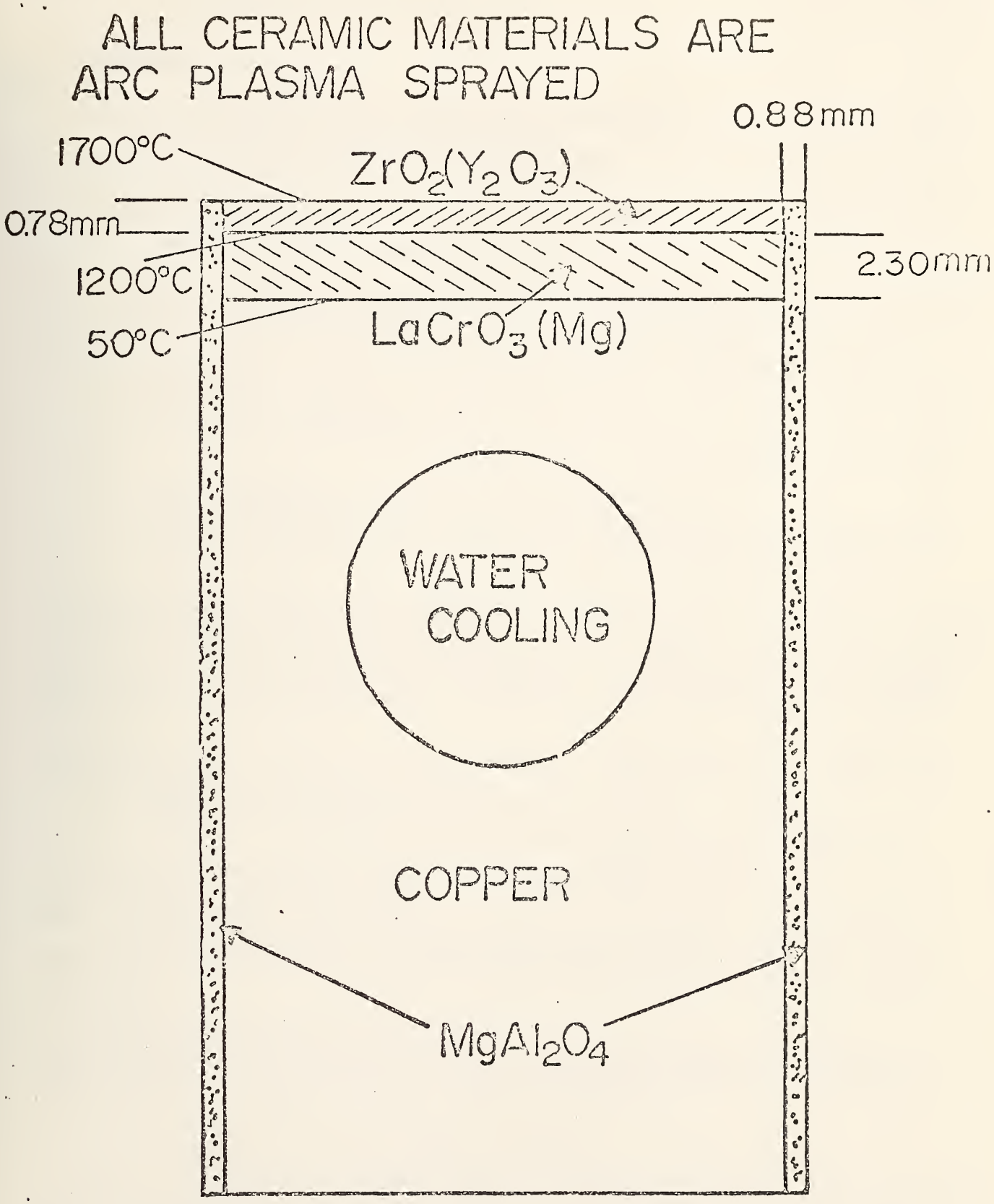

Fig. 1. Schematic diagram of ZrO_2/Y_2O_3-$LaCrO_3$ electrode.

c. Technetics Spinel Electrodes (T. Negas)

Introduction

Spinel-based electrodes fabricated by Technetics are shown schematically in Fig. 2. Construction materials include,

a. Spinel solid-solution, $75MgAl_2O_4:25Fe_3O_4$ as the conducting ceramic, arc-plasma sprayed.

b. Fe/Cr alloy mesh (plus smaller amounts of Al, Si and Ni) brazed to Cu as the leadout complex.

c. Sintered $MgAl_2O_4$ insulators not bonded directly to the electrode complex.

These electrodes were tested by ANL at the Reynolds Research Laboratories on October 27, 1976. Test conditions are summarized below.

a. 5:09 pm, 10/27/76, start-up, after 5-10 min. surface temperature below 800-900 °C;

b. Temperature raised in 4 hrs. from ∿900 °C to 1300 °C, Q ≃ 55-60 W/cm^2;

c. Maintained overnight;

d. 11:45 am, 10/28/76, seed flow started, voltage applied, J up to 1.5 A/cm^2;

e. Arcs on cathode, temperature increased by ∿100 °C;

f. Test condition maintained 1 hr. whereupon arcing became more intense and concentrated at upstream edge, temperature locally up to 1660-1700 °C;

g. Field and seed shut-off at 1:15 pm, cool-down began at 2:45 pm.

In early November 1976, the electrodes were received from ANL whereupon they were "potted" in epoxy and sliced for analytical work. Representative sections were chosen for detailed analysis from slices in the vicinity of the middle portion (see Fig. 2) of anode and cathode. A detailed report (26 figures) is available but will not be reproduced here. The summary below illustrates the scope of the work.

1. The mechanical integrity of the arc-plasma sprayed spinel was compromised during the test.

a. Spalling of the material is particularly evident at the anode.

b. Arcing at the cathode probably enhanced the mechanical degradation.

2. Mechanical degradation combined with poor contact between electrode and insulator (not bonded initially) contributed to considerable penetration of seed, particularly at the cathode.

a. The original spinel and Fe/Cr/Al-wire mesh suffered extensive chemical alteration at the leadout area. The spinel also degraded adjacent to the insulators.

3. Evidence for exsolution of iron oxide from the spinel at the leadout zone was noted. This should be avoided by preventing oxidation (maintaining high density and/or using suitable oxides as dopants.)

d. GE Electrode Test at MIT (T. Negas)

We received (December 1976) an electrode pair from a test conducted at MIT by GE and ANL. Test conditions obtained from ANL include, 11:24 am - start, 12:00 at test temperature 12:08-15:08 at test condition, gas = 2200 K, 1600 °C surface temp., measured Q = 110-150 W/cm^2. Cathode and anode were not labelled nor was a pre-test specimen furnished. Consultation with ANL later established the identity of cathode and anode. GE provides the following declaration:

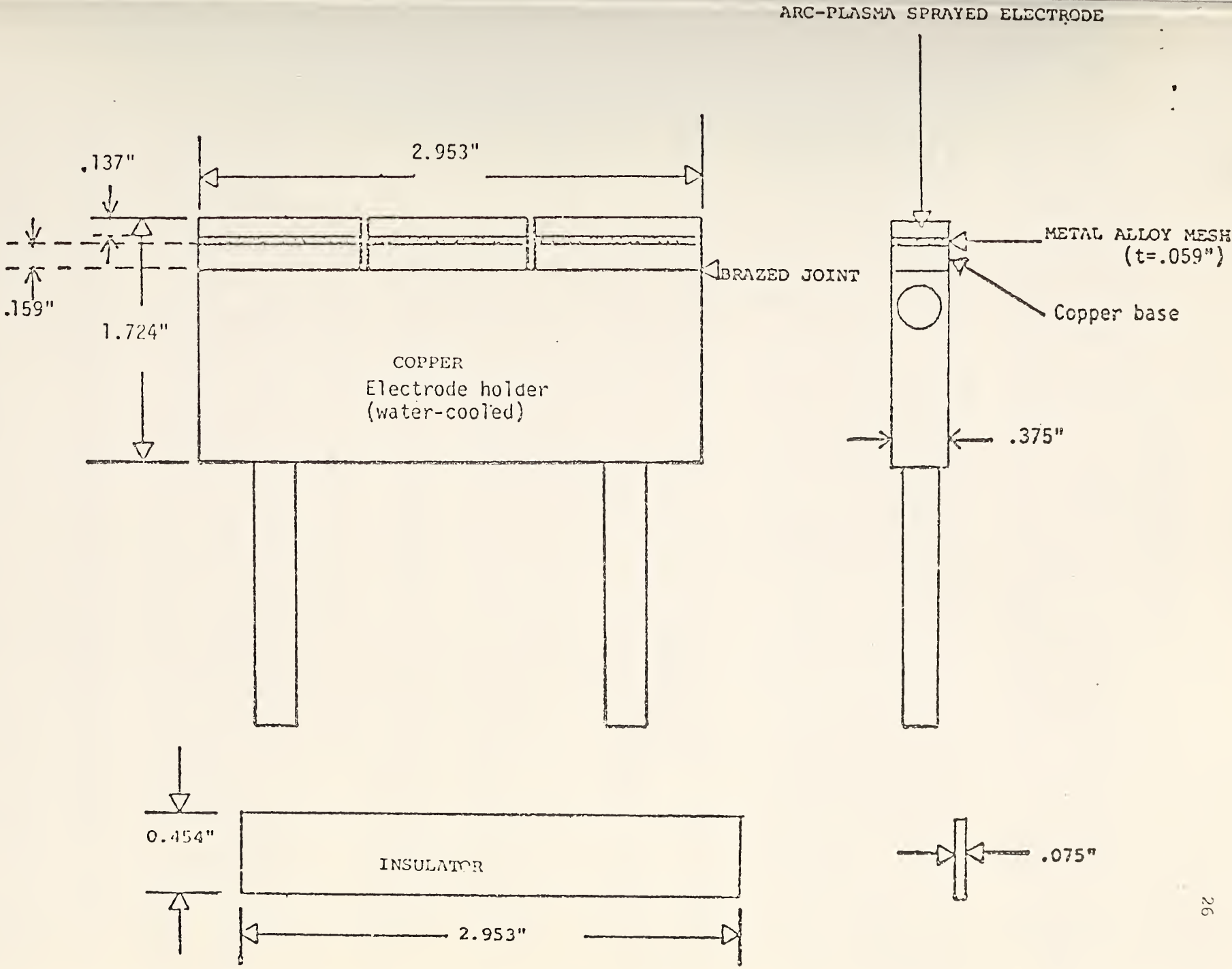

Fig. 2. Design of spinel electrodes for ANL-Reynolds test.

PROPRIETARY NOTICE

The General Electric Co. considers its FLEXBED Electrode Design to be proprietary and the General Electric Co. is providing Electrodes for test and evaluation purposes only. The FLEXBED Design concept, physical structure and characteristics shall not be willfully disclosed or duplicated without the express written authorization of the General Electric Co. unless the design is available from another source without restriction.

In view of the above, specific compositions of construction materials and special characteristics of engineering design will not be disclosed apart from details promulgated in weekly report #1 to ERDA from ANL, 12/1/76. This report suggests that, "..... electrodes were of 25 m/o Fe_3O_4:75$MgAl_2O_4$.... insulators were $MgAl_2O_4$." X-ray diffraction data for relatively undistrubed materials show that the conductor consists of either a poorly crystalline spinel or of a mixture of spinel solid-solutions having slight variability in composition. Regardless, the material is not a 25Fe_3O_4-75$MgAl_2O_4$ (solid-solution) but one having a bulk composition lower in iron oxide content. The insulators are richer in the MgO component than $MgAl_2O_4$.

A detailed report (15 figures) is available but will not be reproduced here. The summary below illustrates the scope of the work. Conclusions based on the available specimens and evidence are summarized by:

a. every attachment involving unlike materials detached during the test,
b. this compromised the original thermal design parameters and led to localized excessive heating,
c. in turn, the spinel conductor melted locally, perhaps fluxed by oxidized Mo and intrusion of potassium,
d. the use of Mo-containing construction materials (or, in fact, Cu-metal) for temperature regimes certainly above 500 °C, in our opinion, becomes overly optimistic; oxidation of these components, even locally, will cause detachment of the electrode and its ultimate destruction,
e. the spinel electrode either exsolved iron oxide during operation or during fabrication; for either case, a more resistive phase assemblage would be localized at the critical metal-ceramic leadout zone.

3a. AVCO, Copper-Boron Nitride-Slag Cathode (T. Negas)

We received from AVCO an electrode system (cathode wall) consisting of two grooved copper frames insulated by boron nitride (BN). Grooves were filled with an "alumina"-based castable. The electrodes were operated with seed plus slag for ~20 hours. Low resistance developed between copper frames during operation but remained high after cool-down. Possible reasons for axial leakage, therefore, were investigated. A final report (39 figures) is available but will not be reproduced here. The summary below illustrates the scope of the work.

Figure 3 illustrates the Cu-BN-castable-slag electrode complex. The following conclusions can be derived from the analysis:

1. Slag is differentiated into three primary zones, perhaps somewhat modified during cool-down.
   a. The basal slag is glassy and probably did not crystallize at operating temperatures during the test duration. It probably represents the "coldest" slag, being associated only with the Cu-ridges and BN. Alternatively, it may

be argued that this slag was cold but, nevertheless, entirely fluid during operation. The high K-content presumably could lower crystallization temperatures especially if the underlying BN oxidized and was incorporated.

2. The middle slag zone is partly crystalline, containing an Fe-rich phase.

3. The uppermost slag zone is porous and glassy (molten during the test) as expected.

4. The Al/Si-rich castable degrades via reaction of K primarily with Si.
   a. This suggests that Si is selectively leached or fluxed by K, a phenomenon borne out by past laboratory experience. K/Si-liquid phases can form at temperatures <700 °C. The materials are ionic conductors as shown by numerous studies in the past.

5. Debris between the slag and Cu-BN-castable complex consists primarily of K/Al/Si-oxide phases apparently derived from the castable and, perhaps, the slag. Slag components such as Fe and Ti are not present.

6. The BN was penetrated by K and, possibly, products from reactions among K, Al and Si-oxides.
   a. Some of theAl and Si may have been derived from castable incompletely cleaned from above the BN during fabrication of electrodes.

7. A zone of acid-soluble materials is located at the slag/Cu-BN castable interface.

Based on these observations, possible causes for axial leakage can be attributed to:

1. Condensed seed plus conductive fluids rich in K/Si-oxides derived primarily from the castable and possibly from the slag.

2. The upper two slag zones (Fe-rich crystals plus liquid and liquid) may be connected electrically by the castable.

3. Within the castable K-rich and K-Si-oxide rich fluids could complete the circuit when in contact with the adjacent Cu.

Possible design changes to remedy the problem include:
1. Use a castable without SiO_2 as a dominant component.
2. Completely leave out the castable in the electrode design (also the Cu-grooves) in which case slag will not "stick" to Cu or BN.

b. Testing at AVCO (W. R. Hosler)

A program for testing materials in slagging environments has been initiated with AVCO Everett. The goal is to find a material or combination of materials that will withstand the stresses under MHD conditions. The principal concerns are the erosion and corrosion of materials due to arcing and chemical interaction with coal slag as well as the problems of shorting the Hall voltage across the insulators along the length of the channel.

The initial designs incorporate generally the use of magnesium aluminate ferrous ferrite (MAFF 31) bonded to the standard AVCO Mark VI copper channel base. Bond types using both metal mesh and cermets will be used to attach the MAFF 31 to the metal base. In some cases, the electrodes will be capped with coal slag applied by arc plasma spraying before run initiation.

The copper base electrodes (22) have already been received from AVCO. Specific designs have been made and will be fabricated as soon as funding details can be arranged.

B. Joint US-USSR Test of Soviet Materials at UTSI (Phase II) (A.J. Armstrong)

During the period February 14-18, 1977, five Soviet scientists together with their colleagues at the University of Tennessee Space Institute performed a series of experiments to explore the effect of coal slag on various high temperature electrode materials under electric field conditions. Four runs were made in the UTSI II MHD test channel. A. J. Armstrong of NBS participated in the tests. These tests were very similar to the corrosion tests (Phase I) reported in NBS-ERDA Quarterly Report #6 (Dec. 31, 1976) with the addition of an externally applied current. The tests consisted of two runs with acid coal and two runs simulating basic coal. All four runs used K_2SO_4 seed and an externally applied electric field of 1.0 A/cm^2 across each pair of electrodes. The duration of the tests was between 43 and 60 minutes burning coal.

The same two Soviet materials tested previously in Phase I (SiC + 7 wt.% Ti and 60 wt. % $LaCrO_3$ + 40 wt.% Cr) were tested under current in Phase II. Preliminary post-test evaluation indicates that the $LaCrO_3$ + Cr cermet is more resistant to attack by both acid and basic slags. Observation of the voltage-current relationship during and after each run indicates a large current flow (shorting) through the slag when a stable slag layer is obtained.

C. SEM Examination of Specimens Tested at FluiDyne Eng. Corp. (E.N. Farabaugh)

Characterization of materials tested at Fluidyne Eng. Corp. is continuing. Special attention was paid to rebonded Corhart material designated RX-317. This is fused cast material which has been ground and rebonded using other two phase (spinel-magnesia) material. These materials were tested for 30 hours in the presence of seed and ash and without seed or without ash. They were tested typically by cycling between 1800°/1600 °C. A detailed report, summarized below, is available.

Analysis of the rebonded material revealed varying depths of penetration of Ca, K, and Si. The paths for the penetration being around the larger grains of the original X-317 material and through the less dense spinel-magnesia bonding material. Some magnesia phase was found close to the exposed surface of the tested materials. Magnesia had not been found so close to a tested exposed surface before. Thus, for the rebonded material, the K, Si, and Ca did not give rise to a uniformly thick reacted layer found typically in the fused cast material.

One fused cast specimen was examined, FN-95. It was tested at 1800°/1600 °C for 30 hours in the presence of ash but no seed. This specimen showed a densified reacted layer. The densification could have been caused by new Si-Ca-Mg phases forming. This was the first specimen to exhibit such densification.

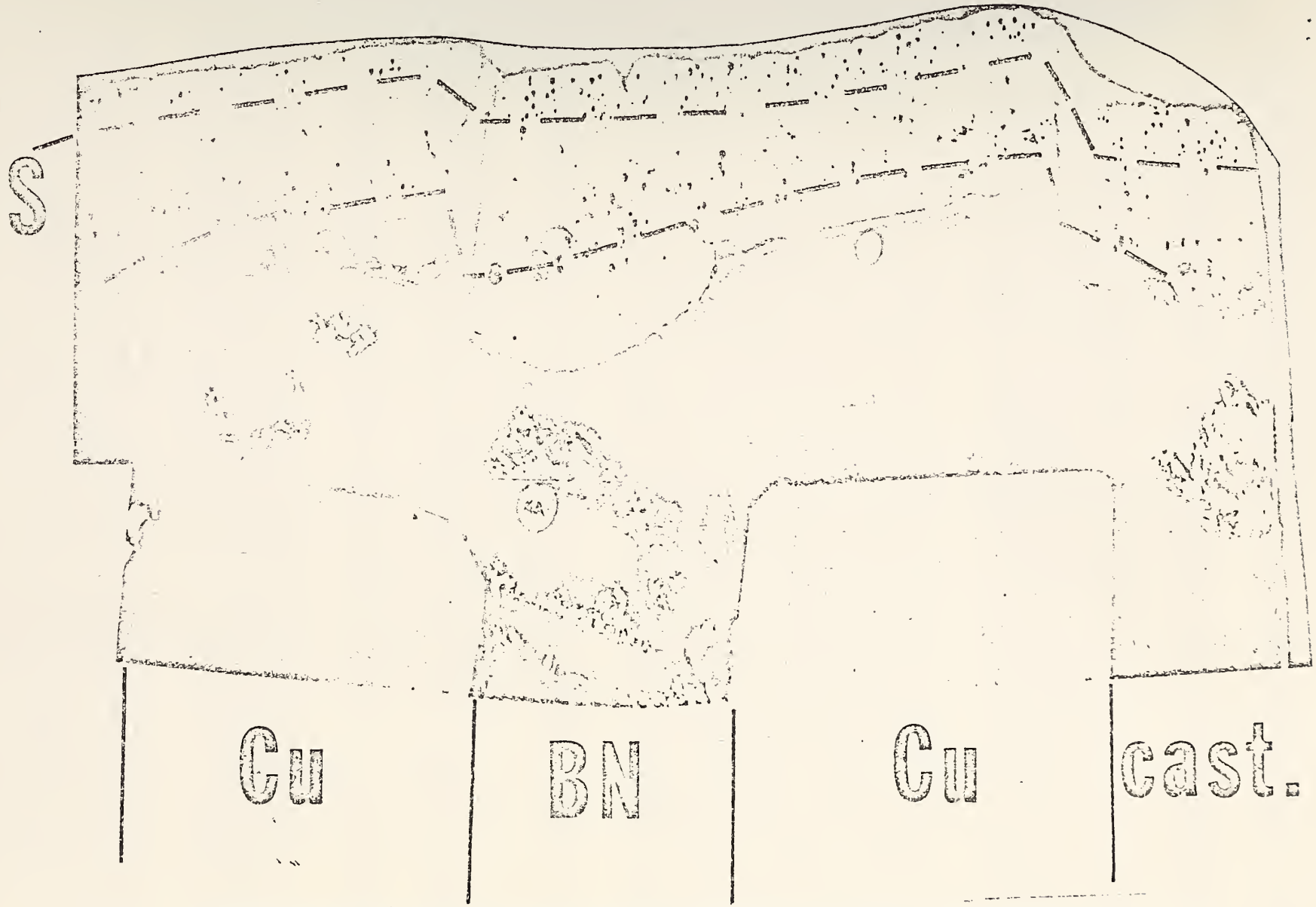

Fig. 3. SEM micrograph (20X) showing Cu-BN-Cu-castable plus slag, AVCO cathode. S = slag (differentiated into three zones, dashed lines); E = epoxy; Cast. = castable.

The next materials to be examined will be a series of magnesia chromite samples tested under conditions similar to those conditions which the X-317 and RX-317 materials were subjected to.

D. Thermal Evaluation of a $3MgAl_2O_4:Fe_3O_4$ Arc Plasma Sprayed Composite Electrode (W. R. Hosler and A. J. Armstrong)

Samples of $3MgAl_2O_4:Fe_3O_4$ spinel bonded to Hastelloy B were obtained from Trans Tech. Four samples were heat treated for from 20 to 72 hrs. at 600 °, 700 °, 800 ° and 900 °C in a furnace in an air atmosphere. After heating, the spinel portion of the samples was seen to have changed color from dark grey to a mixture of areas of red and dark grey. The 600 °C sample was ∿50% red, the 700 °C sample was more than 75% red, and the 800 ° and 900 °C samples were more than 90% red.

Under the electron microscope four distinct layers were seen in each sample. Figure 4 shows all four layers which consisted of a layer of spinel (1) above a layer of spinel - Hastelloy B graded cement (2) which was bonded to the Hastelloy B base (4) with a thin ∿20μ layer (3) of Ni-Ti bonding agent. All layers but the Ni-Ti bonding agent layer were physically uneffected (except the spinel as noted above) by the heat treatments. The Ni-Ti layer appeared uneffected on the 600 ° and 700 °C samples. The 800 ° and 900 °C samples showed a large amount of porosity in the Ni-Ti layer. Figure 5 is a photomicrograph of the Ni-Ti layer of the 600 °C sample which is comparable to Figure 6 of the same area of the 900 °C sample. By EDX mapping it was seen that Ni had remained largely in its original position while Ti had diffused throughout the bonding agent layer leaving many small and several large voids behind.

Although none of these samples failed due to fracture through this bonding agent layer; it seems prudent to avoid exceeding a temperature of 700 °C for extended periods of time in this area.

A subsequent test of electrodes of this type, during which a temperature of 500 °C was maintained over the bonding agent layer, showed no apparent weakening of the bond and no cracking along the bonding agent layer.

E. Chemical Properties of $3MgAl_2O_4:Fe_3O_4$ (MAFF 31) Spinel Solid Solution (T. Negas and C. D. Olson)

In view of the flurry of activities (past and current) involving the utilization of so-called MAFF 31 as a conducting ceramic, this section is devoted to elucidating the chemistry of this (and related) spinel material. Chemical properties are exceedingly important to fabrication methods and to the electrical properties of MAFF-31.

Firstly, it must be appreciated that the composition $3MgAl_2O_4:Fe_3O_4$ (solid solution) is only nominal. Here we are not considering site-occupancy of cations vs. temperature, a feature which is largely irrelevant. Fig. 7 illustrates the composition triangle $MgAl_2O_4$ (spinel)-Fe_3O_4 (magnetite spinel)-Fe_2O_3 (hematite). Under relatively oxidizing conditions (e.g., in air, $P_{O_2} \approx 0.2$ atm) the bulk composition $3MgAl_2O_4:Fe_3O_4$ is attained only above 1400 °C. At lower partial pressures of oxygen this temperature, of course, will decrease. The spinel solid solution is cubic with $\underline{a} = 8.195$ Å. Thermogravimetric (TGA) and quenching data indicate that below ∿1400 °C (in

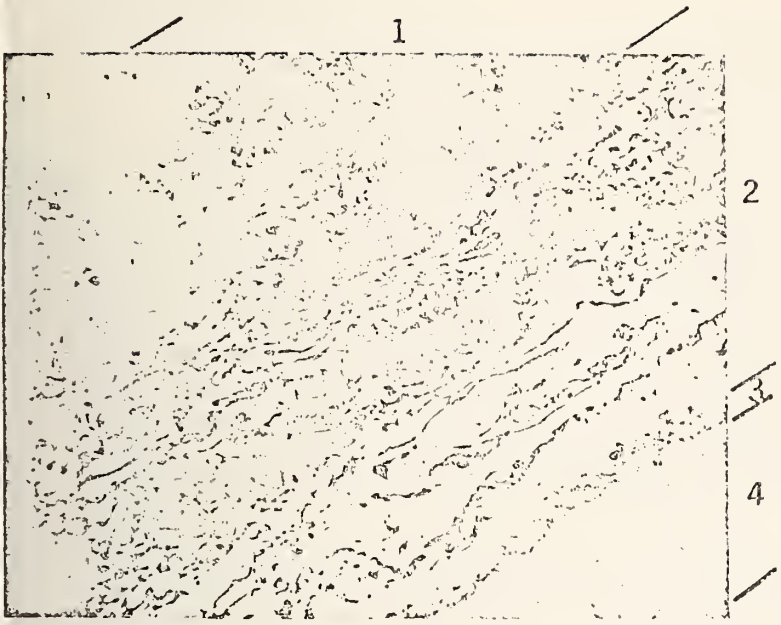

Figure 4 . A 100X scanning electron micrograph of the 800 °C sample showing all four layers.

Figure 5 . A 1600X scanning electron micrograph of the 600 °C sample showing the unaffected bonding agent layer.

Figure 6 . A 1600X scanning electron micrograph of the 900 °C sample showing the large amount of porosity produced in the bonding agent layer.

air), the iron oxide (Fe_3O_4) component oxidizes rapidly and reversibly as a function of decreasing temperature. As the material (in loose, fine powder form with access to available oxygen) oxidizes, the bulk composition (Fig. 7) shifts toward the $MgAl_2O_4$-Fe_2O_3 tie-line. Maximum oxidation is attained below ∿1000 °C and the material can be maintained in oxidized form at lower temperatures (red coloration). At maximum oxidation, in air, the Fe^{2+}/Fe^{3+} ratio decreases to 0.21. The material remains as a cubic spinel but the a-dimension contracts to 8.178 A. These phenomena related to oxidation are not unusual for most spinels and have been reported in the literature frequently. Table 1 summarizes the observed reactions. The conducting spinel reacts with available oxygen below ∿1400 °C (in air) to form oxidized spinels based on solid solutions among $MgAl_2O_4$, Fe_3O_4, and γ-Fe_2O_3 (also a spinel) components. Solid solutions of this type necessarily contain cation vacancies ($\boxed{V}_c$) rather than excess oxygen. These vacancies provide convenient paths for diffusion of Fe.

When the oxidized spinel is annealed for extended durations at low temperatures (<1000°, in air), iron oxide as Fe_2O_3 ultimately exsolves. The resulting assemblage consists of a phase rich in the Fe_2O_3 component and $MgAl_2O_4$ containing less iron oxide than the original material. Exsolution thus produces a phase assemblage more resistive than the original single phase spinel solid solution. Prior to exsolution an oxidized spinel with metal vacancies can exist at low temperatures. This oxidized spinel based on γ-Fe_2O_3 may have a significant conductivity based on Fe-cations migrating through available vacancies. For the $3MgAl_2O_4$:Fe_3O_4 spinel, the reactions related above can be avoided by retaining the ceramic body in dense crack-free form (i.e., minimize diffusion of oxygen). Similar reasoning is applicable to "hercynite"-based spinels. TGA data derived from dense MAFF 31 prepared by Trans-Tech, Inc. indicate that oxidation is effectively negated.

How does this discussion correlate with the electrical conductivity measurements published for MAFF-31? In the first place the four-probe method was utilized combined with high density ceramic bodies. Response to P_{O_2} variation was minimal. This, however, must be expected as the material was maintained in dense, crack-free form and, therefore, not permitted to undergo equilibrium oxidation. Although the conductivity of MAFF-31 was measured the conductivity of oxidized variants of MAFF-31 cannot be determined by the imposed experimental methods. However, oxidation phenomena are clearly evident in the less dense "NAFF" and "MAFF-11" materials given in this report (Task I. Electrical Conductivity).

It also should be appreciated that for MAFF-31, exsolution to more resistive phases requires durations exceeding ∿1 week at temperatures <1000 °C (air). The U-02, Phase II test, 75 hours, however, clearly showed that the MAFF-31 electrodes, primarily cathodes at high current density, exsolved Fe_2O_3 during the short test duration. This suggests that the exsolution process is enhanced electrochemically. Again, an oxidized MAFF-31 containing cation vacancies would be prone to accelerated exsolution via passage of current.

Let us now focus on the methods recently employed to fabricate MAFF-31 electrodes. Figure 8 illustrates features of electrodes fabricated by L. Bates at BNW for U-02, Phase II. Starting MAFF-31 powders were purchased from Trans Tech, Inc. The upper SEM micrograph illustrates the relatively dense

microstructure of the upper portion of a typical electrode. The corresponding line (at right) represents a portion of the X-ray diffraction powder pattern for the dense MAFF-31. It also corresponds with the original Trans-Tech powder which consists of $3MgAl_2O_4:Fe_3O_4$ solid solution, hereafter referred to as reduced MAFF-31. To provide a surface for bonding of a metal leadout (~600 °C interface design, done by Westinghouse Corp.) the porosity of MAFF-31 was enhanced by L. Bates at the lower portion of the electrode, Fig. 8, bottom SEM micrograph. The X-ray lines, at right, show that the lower, porous zone now consists of at least two spinels, the fully oxidized MAFF-31 (based on γ-Fe_2O_3, plus cation vacancies, see Table 1) plus reduced conducting MAFF-31. U-02, Phase II, MAFF-31 electrodes, therefore, contained an oxidized, probably more resistive spinel at the leadout zone prior to the test. Clearly, the increased, controlled porosity at the electrode base enhanced oxidation probably during the cool-down segment of the fabrication process. Exsolution of Fe_2O_3, enhanced electrochemically, necessarily followed during the U-02 test. Significantly, the MAFF-31 cathode that performed for the longest duration (~56 hrs.) was fabricated by Trans Tech, Inc. It was a dense, sintered ceramic without a porous leadout zone.

Another method of fabricating electrodes based on MAFF-31 involves arc-plasma spraying. One design utilizes a porous metal mesh at the leadout zone. MAFF-31 is sprayed onto this mesh. This configuration, in our opinion, invites oxidation of the MAFF-31 at the critical spinel-porous mesh interface. Indeed, the exsolution process (see above) has been observed at this interface for electrodes tested for limited time durations. A second design involves spraying MAFF-31 onto a metal such as Hastalloy B. Specimens of these electrodes were heated overnight at 600, 700, 800 and 900 °C in air. This was done to investigat the metal-MAFF 31 bond line. We obtained these materials to analyze the MAFF-31. Each sample yielded an x-ray powder pattern illustrated by a typical portion in Fig. 9. The pattern consists of a spinel(S) containing less iron oxide than MAFF-31 plus Fe_2O_3 (F). This pattern also is typical for some of the U-02 cathodes (post-test) and for powders permitted to oxidize and exsolve iron oxide under laboratory conditions. Here we have a dilemna summarized below.

1. Powdered MAFF-31 exsolves Fe_2O_3 only sluggishly, requiring ~1 week at temperatures <1000 °C.

2. Dense, sintered MAFF-31 is not susceptible to oxidation and exsolution processes.

3. Arc-plasma sprayed "MAFF-31" oxidizes and exsolves Fe_2O_3 within 20 hours (600-900 °C), no current.

4. Identical starting powders (Trans-Tech) were utilized for the materials noted above.

The above observations clearly point to the arc-plasma spraying process as the medium by which MAFF-31 is left prone to oxidation/exsolution. Two factors can be isolated. X-ray analysis of several, virgin, sprayed specimens of MAFF-31 reveal that the material is characterized by broad diffraction lines. This suggests poor crystallinity and/or poor homogeneity. Sintered ceramics yield x-ray patterns containing sharp x-ray lines indicative of a well-crystallized, ordered material. As the spraying process introduces temperatures far exceeding the melting point of MAFF-31 and as iron oxide is highly susceptible to reduction at these elevated temperatures, it appears hardly likely that the MAFF-31 product would be as chemically and "crystallographically" homogeneous as a carefully sintered MAFF-31. Indeed, the sprayed

MAFF-31, having rapidly crystallized from the liquid phase (and disordered?) may equilibriate more rapidly to the phase assemblage (exsolution products) stable at low temperatures. Alternatively, the sprayed material, although poorly crystalline/homogeneous may contain a second phase such as Fe metal, Fe_3O_4, and/or $Fe_{1-x}O$ (wustite) which serves as the precursor for oxidation to Fe_2O_3 (Fig. 9). The precursor phase need not be entirely crystalline and, hence, not detectable by x-ray diffraction. Evidence for a precursor was obtained from one specimen of MAFF-31 sprayed by Technetics Corp. The X-ray pattern consisted of broad x-ray lines attributed to spinel plus weak, broad lines of a secondary phase. The secondary phase appears to be $Fe_{1-x}O$, wustite.

This discussion illustrates the importance of thoroughly understanding the chemical properties of a material prior to developing fabrication methods and engineering designs. Chemical alteration, particularly via oxidation, is often subtle and difficult to deduce by electron microprobe and SEM/EDX methods (unless exsolution occurs). However, this alteration can lead to the formation of resistive phases (for electrodes) and consequent damage if ignored. For MAFF-31 and related spinels, it is suggested that suitable oxide dopants be utilized to effectively block oxidation, formation of vacancies, and exsolution at low temperatures. These approaches are under investigation.

Table 1. Summary of Generalized Reaction Sequences of MAFF-31 Spinel

$$\left[MgAl_2O_4\text{-}Fe_3O_4\right] + O_2 \longrightarrow \left[MgAl_2O_4\text{-}Fe_2O_3\ \boxed{V}_c\right]$$

SPINEL SOLID-SOLUTION CONDUCTOR

SPINEL SOLID-SOLUTION WITH γ-Fe_2O_3

$$\longrightarrow MgAl_2O_4 + \alpha\text{-}Fe_2O_3$$

EXSOLUTION TO RESISTIVE PHASES

EXSOLUTION WITHOUT CURRENT -- SLUGGISH, E.G., 500°-1000 °C, IN WEEKS

EXSOLUTION WITH CURRENT -- ENHANCED, WITHIN HOURS

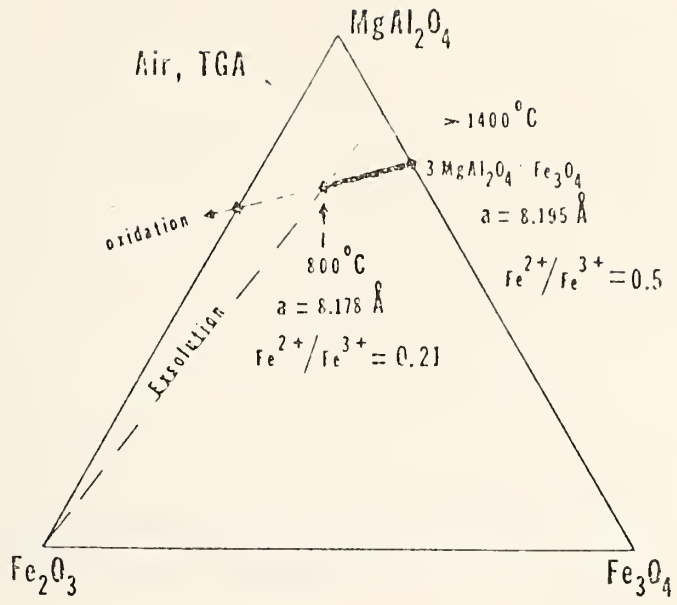

Figure 7. $MgAl_2O_4$-Fe_3O_4-Fe_2O_3 composition triangle illustrating the oxidation, exsolution behavior of $3MgAl_2O_4$:Fe_3O_4 spinel solid-solution (MAFF-31). Data refer to thermogravimetric analysis from 800-1400 °C, in air.

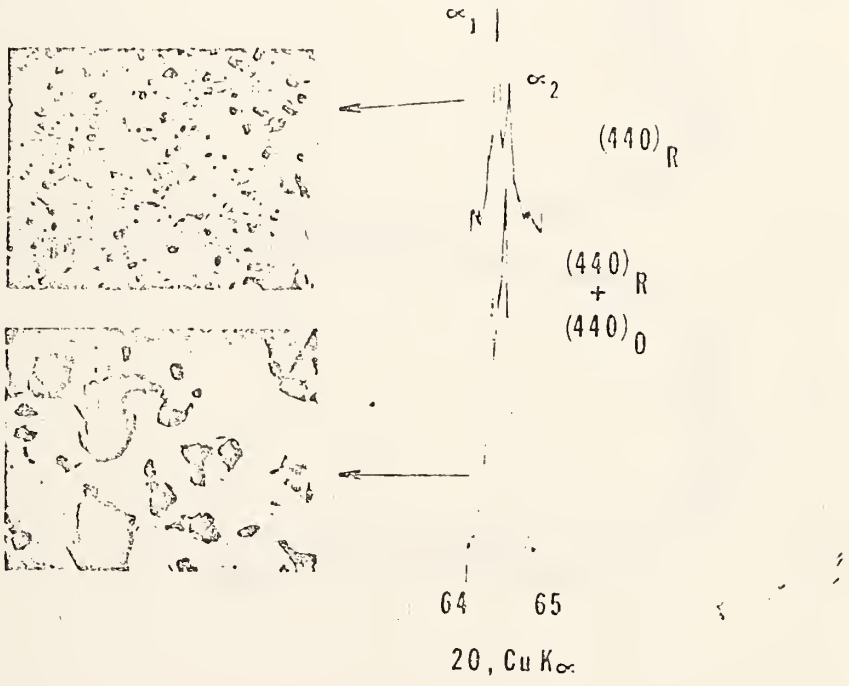

Figure 8. SEM micrographs (original 1000X, reduced by 2/3) and X-ray spectra for MAFF-31 spinel fabricated for U-02, Phase II. Upper micrograph is for the upper dense portion of the electrode while the lower illustrates the more porous leadout area. The selected x-ray lines correspond with the material in each micrograph. The (440) spinel line is shown; R = reduced MAFF-31; O = oxidized MAFF-31.

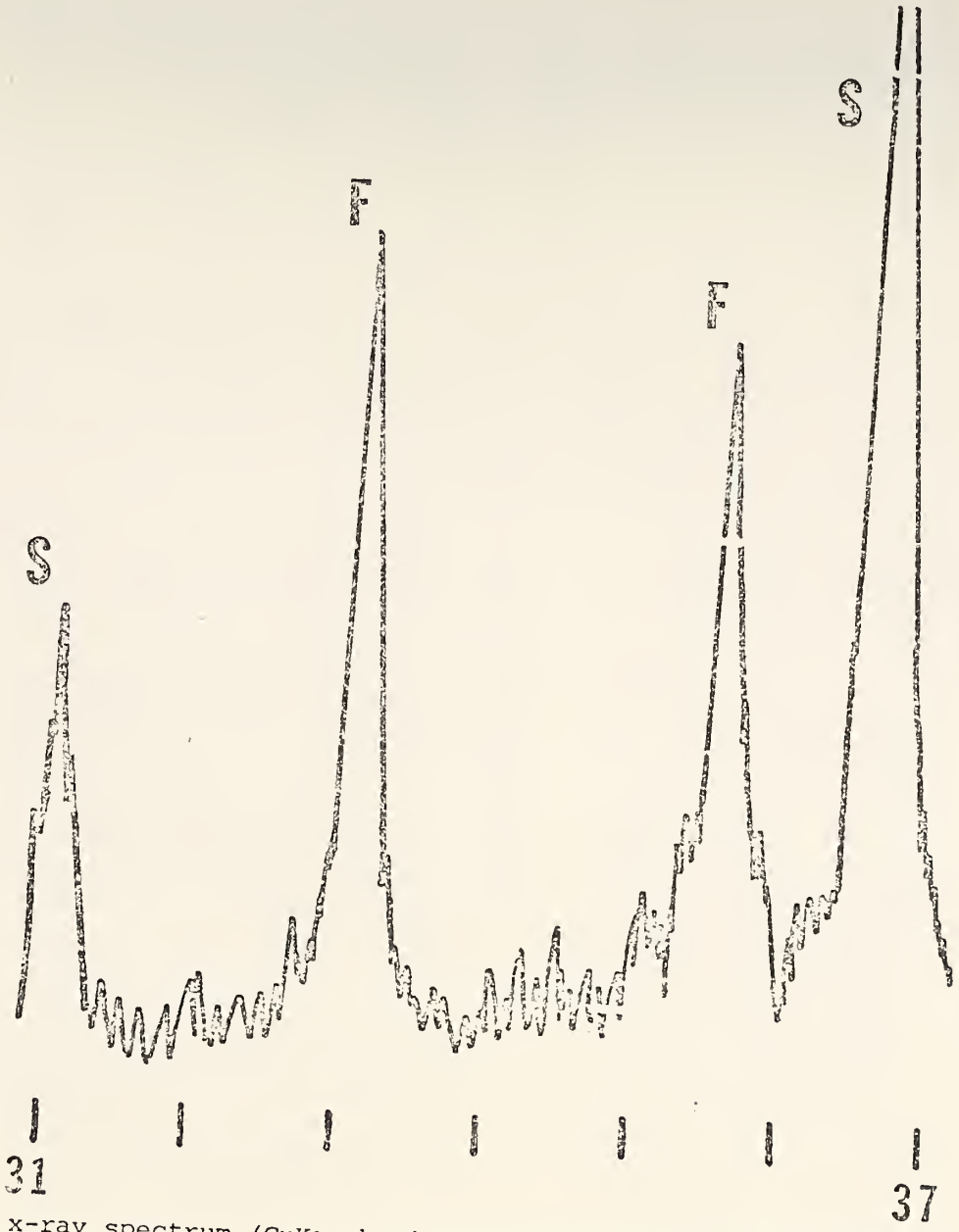

Figure 9. Portion of x-ray spectrum (CuKα, horizontal scale in 2θ) representative of exsolution products of powdered MAFF-31 spinel and of annealed (600-900 °C, air) arc-plasma sprayed MAFF-31. S = spinel; F = Fe_2O_3.

Task L. ASSESSMENT OF STEAM PLANT COMPONENT (J. R. Cuthill)

This is the 7th quarterly report since the initiation of Task L. Included in this report is (1) an update of the Table 8-1, "Mechanical Properties" that was presented in the quarterly report for Oct-Dec. 1975; (2) attempt at a ranking of selected alloys in the order of their relative resistance to hot corrosion attack; (3) conclusions to date on the assessment of alloys for the steam heat-exchanger tubes; and (4) coatings for protection against hot corrosion and high-temperature oxidation.

Update of Table of Mechanical Properties

Table 1 is an update of Table 8-1, "Mechanical Properties" in the quarterly report for Oct.-Dec. 1975; the property values have been obtained from various sources (1), (2), (3), (4), (5) and all values have been converted to S.I. Units with appropriate rounding. All of the alloys in the Table are wrought alloys selected with the steam superheater tubing application in mind, with the exception of WI 52 and FSX-418 which are cast alloys. The latter two alloys had been included in Table 8-1 in the earlier report only because in that same report they were cited in a discussion of alloy composition vs. hot corrosion and high temperature oxidation behavior. Table 2 lists the compositions of the alloys in Table 1 and is also an update of the earlier table.

Relative Resistance of Selected Alloys to Hot Corrosion

A considerable effort was spent this quarter in trying to establish a relative ranking of selected alloys, in respect to their resistance to hot-corrosion attack with the steam superheater application in mind. However, the data is such that a very satisfying relative ranking cannot be made. The data in the literature have been obtained under widely varying conditions of hot corrosion attack under different test conditions, including marine gas turbine test rigs, simulated MHD ducts, crucible immersion tests, and potentiometric measurements, etc. There are even diametrically opposite results frequently reported in hot corrosion literature. Of course, most of the hot corrosion data in the literature are in connection with marine gas turbine research. [A review of a number of comparisons of superalloys for gas turbines, in regard to their hot corrosion resistance, is contained in a report by John Stringer (11)]. However, the gas turbine literature does not include the austenitic stainless steels. This makes it particularly difficult to mesh the stainless steel data from the MHD simulation tests (12), (13) with the superalloy data.

With this background, a ranking of those alloys included in Table 1, is attempted in Table 3. The listing is in order of decreasing resistance to hot corrosion attack.

It is quite evident that Inconel 671 as a cladding, or the equivalent, would be a first choice, as far as resisting hot corrosion attack is concerned, and that the low chrome-moly steels that formerly were widely used for boiler tubes would be at the bottom, but the problem is in the middle in meshing the group of stainless steels relative to the group of superalloys having intermediate resistance to hot corrosion. For this reason the listing

is divided into the two columns.

The stainless steels present another problem. Type 316 and to a lesser extent type 310 are subject to carbide precipitation upon slow cooling after prolonged service in the range in which the steam heat-exchanger tubing will be operating (1100-1200°F). This tendency for carbide precipitate formation is minimized or eliminated by using the low carbon version of these stainless steels, i.e. type 316L or 310L. (1).

Conclusions to date on Assessment of Alloys for Steam Heat-Exchanger Tubes

Review of relationships between alloy composition and resistance to hot corrosion attack, as discussed in previous quarterly reports, has lead to the following conclusions as to composition guidelines to follow in judiciously selecting alloys expected to have good hot corrosion resistance:

1. Hot corrosion resistance increases with increase in chromium content, and is very sensitive to chromium content (see Figure 1). Alloys that depend upon a chromium oxide protective film for their corrosion resistance are the best for resisting hot corrosion.

2. Avoid alloys that depend upon an Al_2O_3 protective film for their good temperature oxidation resistance.

3. Avoid alloys high in tungsten and molybdenum added as carbide formers. Their carbides at the surface act as nucleation centers for hot corrosion pitting.

4. The combination of chloride and sulfate is disporportionately worse than sulfate alone.

5. Data on attack by sodium salts gives a first approximation to what might be expected from molten potassium salts.

6. The ambient flue gas composition is sufficiently critical in respect to the severity of the hot corrosion attack that a test, in a rig that simulates the service condition as closely as possible, should be conducted before the final choice of alloy is made.

7. A material such as INCO 671/800H clad tubing would be a first choice of material for the superheater tubing in respect to the certainty of resisting the hot corrosion attack, providing an oxidizing atmosphere is maintained. A less expensive material may prove to be adequate but a simulation test in a burner rig is recommended, when the anticipated gas composition is better known, before such a choice is made.

Coatings for Protection Against Hot Corrosion and High-Temperature Oxidation

An alternate method of achieving adequate corrosion resistance is by coating.

Chatterji, DeVries, and Romeo in a recently published review (7) list some, - in the authors words, - "popular commercial coatings" to resist high temperature oxidation and hot corrosion. This list is reproduced in Table 4. These coatings fall generally into two classes (1) diffusion coating or surface case that is usually achieved by a pack cementation process similar to pack carburizing, and (2) overlay cladding in which the alloy generally is applied either as (a) a slurry, or "slip", dried and fired, or (b) as a powder by a plasma spray gun.

Figure 2 shows results of Bartocci (8), reproduced by Chatterji, DeVries, and Romeo in their Review. The data shows the beneficial effect of the coatings marked with an asterisk in Table 4 in protecting IN-713 against hot corrosion in burner rig tests. The coatings were applied by the pack cementation process.

A method of coating application not discussed by Chatterji, DeVries, and Romeo is the use of a high power laser beam to melt a thin surface layer while adding the desired alloying element into the molten region. Surface layers containing up to 50% Cr are reported to have been produced in steel by AVCO Everett Research Laboratories, Inc., using the 15kW, CO_2 laser equipment which they have developed (9), (10).

References

1. Aerospace Structural Metals Handbook, Vols. 2, 4, and 5, 1976 revision, Mechanical Properties Data Center, Belfour Stulen, Inc., Traverse City, Michigan.

2. Structural Alloys Handbook, Vol. 2, 1977 edition, Mechanical Properties Data Center, Belfour Stulen, Inc., Traverse City, Michigan.

3. "Materials Selector 76", Materials Engineering 82, 4, (1975).

4. Properties Bulletins from Cabot Stellite Division, Kokomo, Ind. 46901.

5. Research reports from Huntington Alloy Products Division, INCO, Huntington, W. Virginia 25720.

6. A. M. Beltran and D. A. Shores, Chapter 11, p. 332, The Superalloys, C. T. Sims and W. C. Hagel, eds., John Wiley, c1972.

7. D. Chatterji, R. C. DeVries, and G. Romeo, Protection of Superalloys for Turbine Application, Advances in Corrosion Science and Technology, Vol. 6, M. G. Fontana and R. W. Staehle, eds., Plenum Press, 1976.

8. R. S. Bartocci, Behavior of High Temperature Coatings for Gas Turbines, Hot Corrosion Problems Associated with Gas Turbines, ASTM-STP-421, 1967.

9. F. D. Seaman and D. S. Gnanamuthu, Using the Industrial Laser to Surface Harden and Alloy, Metal Progress, 108, (3), 67-74, 1975.

Table 1

Alloy Compositions

C = cast material
W = wrought material

Resists v. hi-temp oxidation

Resists molten sulphate

Base Alloy Type

Carbide formers

	UNS No.*	Mfgr. Desig.	Cr	Ni	Co	Fe	Al	Ti	Zr	Hf	V	Nb	Ta	Mo	W	Mn max	Si max	C	Other
		Haynes 25	19-21	9-11	bal.	3.0 max	-	-	-	-	-	-	-	-	14-16	1-2	1.0	0.1	
W	S31000	310 S.S.	24-26	19-22	-	bal.	-	-	-	-	-	-	-	-	-	2.0	1.5	0.25 max	0.045P max
W	S31600	316 S.S.	16-18	10-14	-	bal.	-	-	-	-	-	-	-	-	2.0-3.0	2.0	1.0	0.08 max	0.045P max
W	S44600	446 S.S.	23-27	-	-	bal.	-	-	-	-	-	-	-	-	-	1.5	1.0	0.2 max	0.25 max N 0.040 max
C	N07713	IN713C	12-14	bal.	-	2.5 max	5.5-6.5	0.5-1.0	.05-.15	-	-	1.8-2.8	-	3.8-5.2	-	.25	0.5	0.12	.005-.015
W	N07500	U500	15-20	bal.	13-20	4.0 max	2.5-3.2	2.5-3.2	-	-	-	-	-	3.0-5.0	-	-	-	0.15 max	.008 B max
C		FSX418**	29.5	10.5	bal.	2.0	-	-	-	-	-	-	-	-	7.0	1.0	1.0	0.25	0.012B
C		WI-52	21.0	-	bal.	-	-	-	-	(Nb+Ta)		= 1.75 total		-	11.0	max	max	0.45	0.15 Y
W		INCO Clad 671/800H	see below for compositions of cladding (671) and substrate (800H)													0.50 max	0.50 max		
W		Inconel 671	48.0	bal	-			0.35										0.05	
W		Incoloy 800H	21.0	32.5	-	46.0	0.38	0.38								0.75	0.50	0.08	0.38 Cu 0.008 S

*The Unified Numbering System (11) is a consensus system of alloy identification covering all commercially produced metals and alloys within the United States. The system was developed and is administered by a committee representing standards organizations, metal and alloy producers, and government agencies including the National Bureau of Standards. The Unified Numbering Systems provides a means of correlating many and diverse nationally used numbering systems.

**Cast alloy - not commercially available.

Table 2

Mechanical Properties*

	1000 hr. Rupture Strength MPa($10^6 N/m^2$)	Yield Strength .2% offset, MPa	Tensile Strength MPa	Elastic Modulus $x10^3$Pa($10^9 N/m^2$)	Creep Strength 1% elongation at 10,000 hr. MPa	Fatigue Str. 10^8 Cycles MPa	Charby Y-no Impact Strength Joules
Haynes 25	124 (816°C)	238 (871°C)	322 (871°C)	181 (760°C)	172 (640°C)	83 (982°C)	163 (871°C)
310 S.S.	172 (593°C)	138 (593°C)	448 (593°C)	200 (RT)	103 (649°C)	217 b RT	121 (RT)
316 S.S.	241 (593°C)	172 (593°C)	414 (593°C)	193 (RT)	83 (649°C)	269 b RT	106 (RT)
446 S.S.	39 (593°C)	155 (593°C)	442 (593°C)	200 (RT)	17 (593°C)	324 b RT	2.7 I (RT)
M713C	448 (760°C)	304 (982°C)	469 (982°C)	148 (982°C)	59 (927°C)	179 (649°C)	10.8 (649°C)
U500	145 (871°C)	241 (982°C)	317 (982°C)	142 (982°C)	69 (871°C)	331 (816°C)	10.8 (649°C)
FSX418***	NA	NA	NA	NA	NA	NA	NA
WI-52	103 (927°C)	276 (871°C)	414 (871°C)		138a (871°C)		
INCO Clad 671/800H	**	**	**	**	**	**	**
Inconel 671	97 (649°C)	290 (649°C)	552 (649°C)	**	**	**	**
Incoloy 800H	69 (732°C)	100 (649°C)	343 (649°C)	139(816°C)	117* (649°C)	207 (649°C)	244 (649°C)
					a-at 1000 hr	(b) for 10^6-10^8 cycles	I-Izod Impac

*Property values correspond to the temperatures given in parentheses after the value in each case. These temperatures have been selected in most cases because they are either the maximum temperature reported at which the alloy could be used under MHD conditions, or the highest temperature at which data is given.

**The thickness of the alloy 800H substrate only should be used in determining design stresses.

***Cast alloy - not commercially available.

10. Private communication, D. S. Gnanamuthu, AVCO Everett Research Laboratory, Inc., Everett, Mass. 02149.

11. J. F. Stringer, High Temperature Corrosion of Aerospace Alloys, AGARDograph No. 200, August 1975, NTIS Cat. No. AD/A-016095, Nat. Tech. Info. Service, Springfield, VA. 22161.

12. D. Bienstock, R. J. Demski, and R. C. Corey, Corrosion of Heat-Exchange Tubes in a Simulated Coal-Fired MHD System, J. of Engineering for Power, ASME Trans. 93, Series A, No. 2, 249-256.

13. J. B. Heywood and G. J. Womack, Open Cycle M.H. D. Power Generation, pp. 716-721, c1969, Pergamon Press, Oxford.

Table 3. Relative ranking of some selected alloys in decreasing order of resistance to hot corrosion attack.

		Inconel 671
		Haynes 25
		FSX - 418
310 S.S.	‖	U500
316 S.S.	‖	WI-52
446 S.S.	‖	IN-713
		Croloy 9 (9Cr-1Mo steel)
		Croloy 2 1/4 (2 1/4 Cr-1Mo steel)
		Croloy 5 (5Cr-.55Mo steel)

Table 4. Some Commercial High-Temperature Coatings for Superalloys (from Ref. 7)

Designation	Vendor	Coating constituents	Process
NC101A	Sylvania	Al-rich	Pack cementation
ASC-HI-15	Alloy Surfaces	Al-Cr	Proprietary ("vapor deposition")
Nicrocoat 110	Wall Colmonoy	Ni-Cr-TiB_2	Slurry
Nicrocoat 130	Wall Colmonoy	Ni-Cr-Si-$TiSi_2$-TiN	Slurry
Type 701	Lycoming Div., AVCO	Al-rich	Vacuum pack cementation
Type 606B	Lycoming Div., AVCO	Cr-Al-Si	Cr plate + hot dip Al-Si
WL-1	Union Carbide	Al-rich	Pack cementation
C-9	Union Carbide	Al-rich (Al-Fe)	Pack cementation
C-12	Union Carbide	Al-rich	Pack cementation
WL-8	Union Carbide	Al-rich	Pack cementation
WL-14	Union Carbide	Al-rich	Pack cementation
WL-4	Union Carbide	Al-Si-Cr	Pack cementation
C-20	Union Carbide	Al-Cr	Pack cementation
C-3	Union Carbide	Al-Ni	Pack cementation
WL-9	Union Carbide	Al-Si	Pack cementation
IAD	Union Carbide	Al	Hot dip
WL-6	Union Carbide	Be	Pack cementation
Calorizing	Calorizing	Al	Pack cementation
Codep A	General Electric	Al-Ti	Pack cementation
Codep C	General Electric	Al-Ti	Pack cementation
Aldip	Allison Div., GMC	Al	Hot dip
Alpak	Allison Div., GMC	Al	Pack cementation
A-11	Martin Metals	Al	Diffusion-annealed CVD
PWA-47	Pratt & Whitney	Al-Si	Slurry
*MDC-1	Misco Precision Casting	Al-rich	Pack cementation
MDC-1A	Misco Precision Casting	Al	Pack cementation
*MDC-6	Misco Precision Casting	Cr-Al	Pack cementation
MDC-7	Misco Precision Casting	Al-rich	Pack cementation
MDC-9	Misco Precision Casting	Al-rich	Pack cementation
*UC	Chromalloy	Al-Cr	Pack cementation
SUD	Chromalloy	Al-rich (Al-Fe)	Pack cementation
SAC	Chromalloy	Al-Cr-Si	Pack cementation
UDM	Chromalloy	Al-rich	Pack cementation
RT-21	Chromalloy	Al-Cr	Proprietary
RT-22	Chromalloy	Al-Pt-Cr	Proprietary (duplex)
—	TRW	Al-rich	Vacuum pack cementation
—	TRW	Al-Cr	Slurry
—	TRW	Al-Cr	Vacuum pack cementation
SI3-53C	Solar Div., Int. Harvester	Al-Fe	Slurry
S5210-2C	Solar Div., Int. Harvester	Ba-silicate glass + additives	Glassy refractory
S6100M	Solar Div., Int. Harvester	Modified S5210-2C	Glassy refractory
NBS A-418	NBS	Frit 332 + Cr_2O_3	Glassy refractory
MAL-2	Vitro	Al-rich	Electrophoresis
Sermetel J	Vitro	Al-rich	Electrophoresis
BB	Chromizing	Rh-Al	Proprietary
LDC-2	DEW (Germany)	Pt-Al	Electroplate pack cementation

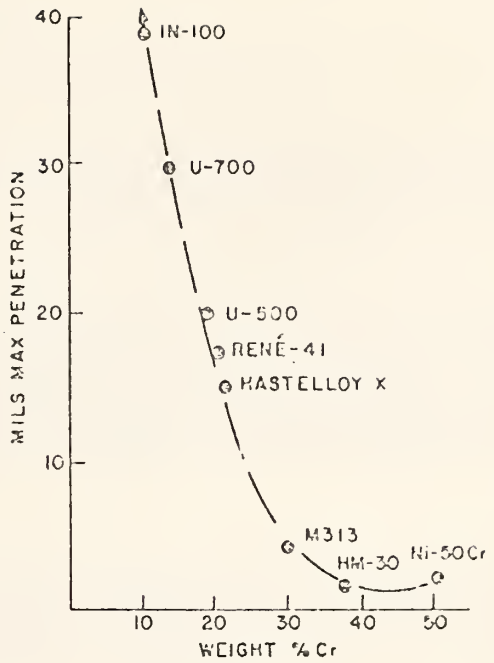

Fig. 1. Hot-Corrosion resistance vs. chromium content of some nickel base balloys (from Ref. 6)

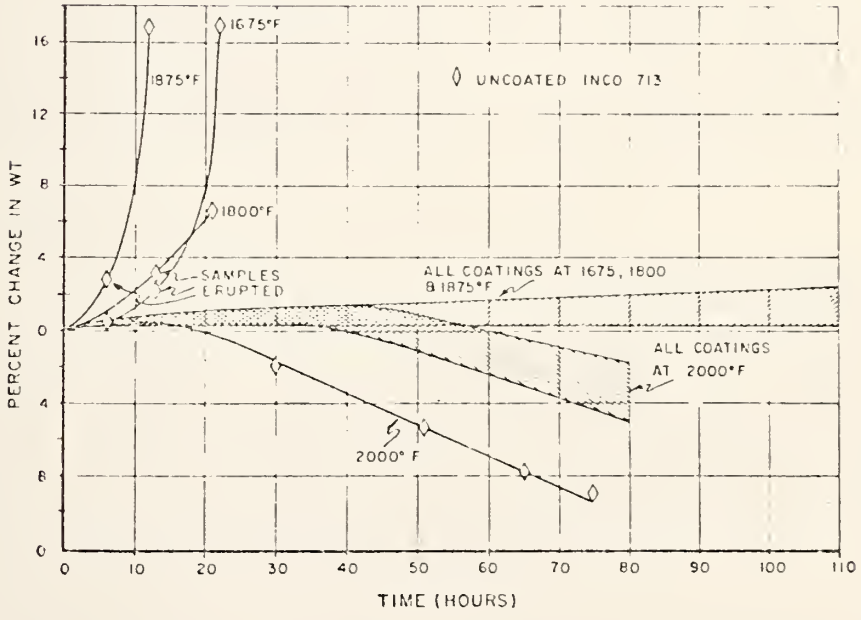

Fig. 2. Coated vs. uncoated IN-713 in resisting hot corrosion in burner rig tests. Coatings include those marked by an asterisk in Table 4. (from Ref. 8)

SUMMARY AND CONCLUSIONS

Task I. - Operational Design Properties

Viscosity

The viscosity of Soviet "standard" (Krushnitz) coal slag is ∿100 poise at 1600 °C compared with "average" Rosebud and "average" Illinois #6 (both synthetic) which attain 100 poise near 1400 °C.

Electrical Conductivity

Nickel aluminate ferrous-ferrite spinels may be promising electrode materials in a slagging MHD generator. Oxidation appears to be a problem for this class of spinels as well as those based on $MgAl_2O_4$:Fe_3O_4 solid solutions. Oxidation can lead to formation of a more resistive phase assemblage at low temperatures.

Vaporization

Preliminary measurements of K-pressures over K_2O-Al_2O_3-SiO_2 solutions using mass spectrometer methods indicate the potential for some success. Previous attempts to perform these measurements using a TGA-effusion cell arrangement proved troublesome.

Task J. Corrosion and Diffusion

Seed-Slag Interactions

Reactions among K_2O-Al_2O_3-SiO_2-"FeO_x" (plus MgO, CaO) are under investigation in a systematic manner. For the $KAlO_2$-$KASiO_4$-"FeO_x" subsystem corrosion products of construction materials based on Al/Fe-oxides or crystallization products from slag alone include Fe_3O_4 and K-β-alumina phases containing iron oxide. These constituents could contribute to axial leakage in a slagging generator provided temperature-composition limits are realized. The electrical (electronic and ionic) conductivity of the K-β-aluminas containing iron oxide should be investigated for they may prove to be valuable materials.

Task K. Materials Testing and Characterization

a. Most of the tested electrode/insulator assemblies analyzed to date have one common feature, failure of bonds and/or attachments among unlike materials. For many cases, however, it is difficult to isolate, chemical, thermal and electrochemical effects. Collaboration with all involved laboratories must be encouraged for only "educated guesses" generally can be given. Laboratory and rig tests of the MAFF-type spinels clearly indicate that these materials must be modified within cooler electrode regions to prevent formation of resistive phases. $LaCrO_3$ (MgO), capped with ZrO_2 (Y_2O_3), electrodes offer promise as indicated by recent NBS/Trans-Tech tests at MIT. Development of $YCrO_3$-based materials should also proceed.

b. The AVCO Cu-BN-slag electrodes show considerable promise provided that the axial leakage problem can be solved. Possible causes were suggested but these remain to be pinpointed by additional testing.

Task L. Assessment of Steam Plant Components

Based on accumulated and updated data, selected alloys are ranked with respect to hot corrosion resistance.